



Mafalda Sofia Mendes Beirão Neto Vaz

Impact of formulation and process variables, in technological features of dosage forms for skin delivery

Dissertação de Mestrado em Tecnologias do Medicamento, orientada pelo Professor Doutor João José Sousa e pela Professora Doutora Carla Vitorino e apresentada à Faculdade de Farmácia da Universidade de Coimbra

Julho 2016



UNIVERSIDADE DE COIMBRA

Mafalda Sofia Mendes Beirão Neto Vaz

Impact of formulation and process variables, in technological features of dosage forms for skin delivery

Dissertação de Mestrado em Tecnologias do Medicamento, orientada pelo Professor Doutor João José Sousa e pela Professora Doutora Carla Vitorino e apresentada à Faculdade de Farmácia da Universidade de Coimbra

Julho 2016



UNIVERSIDADE DE COIMBRA

**“Somos o que fizermos dia após dia,
de modo que a excelência não
é um acto, senão um hábito.”**

Aristóteles

Agradecimentos

A finalização de um ciclo de estudos compreende também um encerramento de desafios a nível intelectual e pessoal, que foram ultrapassados com a ajuda de todos aqueles que contribuíram para a conclusão deste projecto e a quem não poderia deixar de agradecer.

Quero expressar os meus agradecimentos aos meus orientadores, Professor Doutor João José Martins Simões de Sousa pelo encorajamento no início desta etapa e por toda a motivação e optimismo com que sempre me brindou.

À minha orientadora Professora Doutora Carla Sofia Pinheiro Vitorino, pela infindável disponibilidade e apoio ao longo de todo este projecto. Agradeço também o seu interesse e visão crítica com que sempre abordou as dúvidas que foram surgindo ao longo do decurso da presente dissertação.

A todos os elementos e funcionários do Laboratório de Tecnologia Farmacêutica agradeço a simpatia e ajuda prestada, principalmente à D. Gina pelo bom acolhimento e às minhas colegas de laboratório Ana Cláudia Santos, Alessandra Ribeiro e Joana Sequeira, pelas contribuições científicas e momentos de descontração.

Gostaria também de reconhecer o Professor Francisco José de Baptista Veiga e a Professora Maria Eugenia Pina pelo acolhimento na Faculdade de Farmácia da Universidade de Coimbra.

Aos meus amigos, estando mais longe ou mais perto, devo um agradecimento por toda a compreensão, apoio, devaneios e força nos últimos dias. À Rita agradeço por toda a companhia, momentos de distração e idas à biblioteca, que contribuíram para a motivação de escrever a presente dissertação. E à Maria, minha companheira de laboratório, devo um enorme agradecimento por toda a ajuda, paciência, disponibilidade, devaneios e amizade que criámos. Este trabalho não seria o mesmo sem ti.

Por último, quero agradecer à minha família, por toda a força e motivação em todos os momentos deste projecto. E ao Rui, por ser o meu verdadeiro groupie, obrigada por toda compreensão, apoio e encorajamento.

Table of Contents

List of Abbreviations.....	7
Abstract.....	10
1. Introduction.....	12
1.1. The Skin – Functions and Structure.....	12
1.1.1. Epidermis.....	12
1.1.2. <i>Stratum Corneum</i> : The Skin Barrier.....	14
1.1.3. The Dermis.....	19
1.1.4. Skin Appendages.....	20
1.2. Skin Drug Delivery.....	21
1.2.1. Routes of Penetration.....	22
1.3. Factors Affecting Skin Permeation.....	23
1.3.1. Physicochemical Properties of the Drug.....	24
1.3.2. Physicochemical Properties of the Vehicle.....	25
1.3.3. Physiological Factors and Skin Condition.....	26
1.4. Dosage Forms Applied to the Skin.....	27
1.5. Non-Steroidal Anti-Inflammatory Drugs.....	29
1.5.1. Ibuprofen.....	30
1.5.1.1. Physical and chemical properties.....	30
1.6. Aims of Dissertation.....	32
2. Pharmaceutical Development of Ibuprofen Hydrogels and Films for Skin Delivery.....	33
2.1. Introduction.....	33
2.2. Materials and methods.....	33
2.2.1. Materials.....	33
2.2.2. Hydrogels Preparation and Characterization.....	33
2.2.3. Films Preparation and Characterization.....	37
2.2.3.1. Adhesive Properties.....	38
2.2.3.2. Mechanical Properties.....	39
2.2.4. <i>In vitro</i> release and Permeation Studies.....	40
2.2.4.1. <i>In vitro</i> Release Studies.....	41
2.2.4.2. <i>In vitro</i> Permeation Studies.....	41
2.2.5. HPLC Determination of Ibuprofen.....	42
2.2.6. Determination of pH.....	42
2.2.7. Ibuprofen Assay in Hydrogels and Films.....	42
2.2.8. Statistical Analysis.....	42
3. Results and Discussion.....	43
3.1. Pre-formulation Studies.....	43
3.1.1. Texture Profile Analysis.....	43
3.2. Optimization of the Formulations.....	46
3.2.1. <i>In Vitro</i> Release Studies.....	47
3.3. Effect of PEG Molecular Weight.....	48
3.3.1. Mechanical Properties.....	48
3.3.2. <i>In Vitro</i> Release Studies.....	50
3.3.3. Determination of pH.....	51
3.4. Effect on Pharmaceutical Dosage Form.....	51
3.4.1. Preliminary Studies.....	51
3.4.2. <i>In vitro</i> Release Studies.....	52

3.4.3. <i>In vitro</i> Permeation Studies.....	53
3.5. The Effect of Adhesive.....	55
3.5.1. Preliminary Studies.....	56
3.5.2. <i>In vitro</i> Release Studies	55
3.5.3. Mechanical and Adhesive Properties	58
3.5.4. <i>In vitro</i> Permeation Studies	59
4. Concluding Remarks.....	62
5. Future Work.....	63
6. References.....	64

List of Abbreviations

A	α -hydroxy fatty acid
AUC	Area Under the Curve
CER	Ceramide
Cox-2	Cyclooxygenase-2
Cv	Drug Concentration in the Vehicle
D	Drug Diffusion Coefficient
dS	Dihydrosphingosine
EB	Elongation to Break
EO	Esterified ω -hydroxy fatty acid
H	6-hydroxysphingosine
H	Hardness
h	Drug Diffusion Path Length
HPMC	Hydroxypropylmethylcellulose
IBU	Ibuprofen
IUPAC	International Union of Pure and Applied Chemistry
J	Flux
J _{ss}	Flux at the Steady State
K	Partition Coefficient of the Drug
K _p	Permeability Coefficient
N	Nonhydroxy fatty acid
NMF	Natural Moisture Factor
NSAIDs	Non-Steroidal Anti-Inflammatory Drugs
P	Phyto-sphingosine
PBS	Phosphate Buffered Saline
PEG	Polyethylene Glycol
Q	Cumulative Amount of Drug Permeated per unit of skin area
Q ₂₄	Cumulative Amount of Drug Permeated after 24 hours
S	Sphingosine
SC	Stratum Corneum
UV	Ultra-Violet
TS	Tensile Strength
TEWL	Transepidermal Water Loss
TPA	Texture Profile Analysis
USP	United States Pharmacopeia

Resumo

A camada mais externa da pele funciona como barreira para muitos compostos o que significa que, apesar das formas farmacêuticas semi-sólidas terem ganho destaque, devido às vantagens que apresentam face às formulações orais, apenas alguns produtos transdérmicos ou tópicos, como o Ozonol, têm sido desenvolvidos para tratar condições de artrite aguda e/ou crónica, inflamações, ou estados febris, usando fármacos anti-inflamatórios que promovem uma acção curta e um tratamento rápido.

O objetivo desta dissertação consiste em desenvolver um filme com base num gel, para a administração de ibuprofeno, de forma a constituir uma alternativa aos produtos já existentes no mercado.

Para isso, foram preparados hidrogéis sob agitação magnética a 25, 60 e 80°C. Os filmes foram obtidos por laminação e secagem dos hidrogéis a 37°C. A análise das propriedades mecânicas e adesivas foram realizadas através do Texturómetro (TA.TX Plus) e os estudos de libertação e permeação *in vitro*, foram efectuados através das células de Franz.

Os hidrogéis contendo 1,5% de Hidroxipropilmetilcelulose (HPMC) e diferentes rácios de propilenoglicol e PEG 400 foram avaliados primeiramente, com base nas suas propriedades mecânicas, demonstrando que a melhor formulação foi preparada com 20% de PEG 400, a 80°C. Após a escolha de melhor formulação base, foram feitos testes experimentais de forma a averiguar como é que o peso molecular do PEG influenciava o desempenho da formulação. Dado aos baixos valores de libertação obtidos pelos hidrogéis, foi feita uma mudança a nível tecnológico da forma farmacêutica, para filmes.

Os filmes eram, globalmente, finos e transparentes e quando testados em ensaios de permeação, evidenciaram que o PEG 200 era o melhor promotor de permeação.

Para otimizar as propriedades adesivas, foi feita uma selecção de adesivos com base na literatura e testes experimentais, sendo escolhidos o quitosano, na proporção de 1:5 (HPMC: Quitosano) e também o Eudragit L30 D-55 num rácio de 1:1.

Os resultados finais demonstram que o adesivo é crucial, para aumentar a libertação de ibuprofeno da formulação, sendo que o Eudragit obteve valores acima do esperado, obtendo resultados ainda melhores do que a referência comercial.

servir de base para um produto promissor, que combine a adesão ao tratamento por parte dos doentes e a capacidade e eficácia de atender a necessidades médicas, ainda não respondidas.

Palavras-Chave: hidrogéis, filmes, ibuprofeno, propriedades mecânicas e estudos de permeação.

Abstract

The outermost skin layer is an effective barrier to many compounds, that means, although semisolid dosage forms have gained interest due to their advantages in comparison to the oral formulations, only a few topical/transdermal products, as Ozonol, have been developed, specifically to treat medical conditions e.g acute and chronic arthritis, inflammation and fever, using non-steroidal anti-inflammatory drugs (NSAIDs) to provide a rapid treatment with short duration of action.

The aim of the present work was to develop a hydrogel based film for skin delivery of ibuprofen, an NSAID, as an alternative formulation to the few products already on the market.

The Hydrogel formulations were prepared under mechanical stirring at 25, 60 and 80°C. Films were obtained from lamination of the hydrogels, followed by drying in an oven at 37°C. In order to perform the mechanical and adhesive properties analysis a TA.TP Plus Texture Analyser was used. Furthermore, Franz cells were used to assess the *in vitro* release and permeation studies.

Hydrogels based on hydroxypropylmethylcellulose (HPMC), in a concentration of 1.5% containing different ratios of propylene glycol and PEG 400, were firstly evaluated based on their mechanical properties. The results obtained, showed that the best base composition was prepared at 80°C and contained 20% of PEG 400, which was then assessed, so as to understand the effect of the molecular weight of PEG on the formulation performance. Due to a low release extent obtained from the hydrogels, a change to film dosage forms was made.

Films presented, in general, a thin, smooth and transparent aspect and the permeation studies indicated PEG 200 as the best permeation enhancer.

To improve the adhesive properties of the film an adhesive screening, was further performed, resulting in the choice of chitosan in a ratio of 1:5 (HPMC: chitosan) and Eudragit L30 D-55 in 1:1 proportion with HPMC.

The final results showed that the presence of adhesive is crucial to promote the ibuprofen release from the films, showing that the formulation with Eudragit led to better

results than the commercial reference, Ozonol. These main findings may provide a basis for the development of a future promising product, combining an improved treatment compliance and efficacy with the ability to fit an unmet medical need.

Key words: hydrogels, films, ibuprofen, mechanical properties and permeation studies.

I. Introduction

I.1. The Skin – Functions and Structure

The skin, the largest organ of the body, represents between 5 to 10% of total body mass in adults and has as main function the protection of internal organs from external agents, like ultraviolet radiation, microorganisms and chemical products. This barrier has also an important role in homeostasis, by regulating body temperature and blood pressure, as a sensory organ, sensing stimulation in the form of temperature, pressure and pain [1].

Human skin comprises four main regions, which are from the skin surface to the deepest: the epidermis, the dermis, and the underlying subcutaneous tissue, the hypodermis (Fig.1).

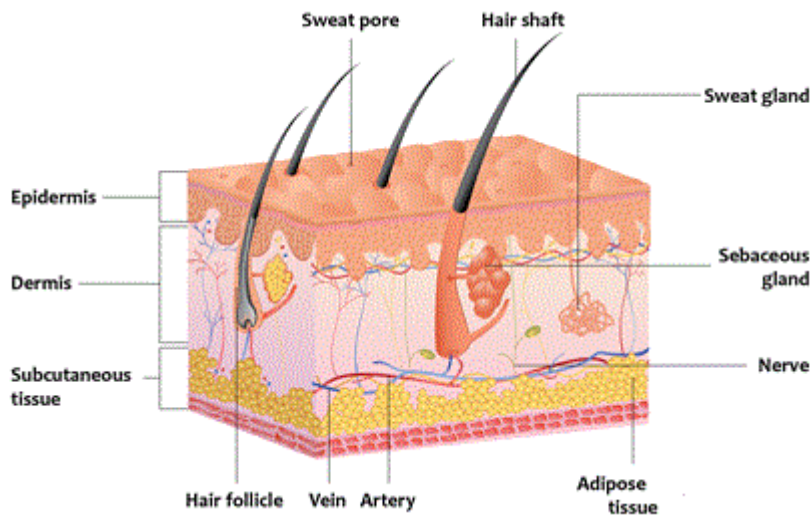


Fig. 1 Representative image of skin layers and components [2].

I.1.1. Epidermis

The epidermis is an epithelium divided into two distinct parts: the viable epidermis, a living hydrophilic layer, which is a stratified epithelium consisting of basal, spinous and granular cell layers, with around 70% of water, and the *stratum corneum* (SC), which is a hydrophobic layer, made from dead cells, with around 30% of water, resulting in a horny texture. With the absence of blood vessels in these layers, the epidermal cells have to source nutrients and remove waste by diffusion across the epidermal to the cutaneous circulation in the dermis.

The epidermis, with about 100 µm of thickness, is a dynamic, constantly self-renewing tissue with formation of a fresh cell layer of keratinocytes at the *stratum basale* and the loss of their nucleus and other organelles to form desiccated corneocytes on their way toward desquamation. In normal skin, this process occurs from the skin surface at the same rate as cell growth in lower epidermis and during their migration, the cells flatten and the protein and lipids that constitute the SC are synthesized. The keratinocyte maturation and desquamation process involves enzymes that are capable of metabolizing topically applied compounds and are also responsible for formation of natural moisturizing factor (NMF) and general homeostasis [3].

Moving from the lower layers upwards to the surface, epidermis consists in the *stratum basale*, also referred to as basal layer or *stratum germinativum*, which contains melanocytes, Langerhans cells, Merkel cells and keratinocytes, the only cells in epidermis that go through cell division.

Melanin is synthesized from tyrosine in the melanosomes, which are associated with the keratinocytes and distributed widely, in order to ensure an even distribution of pigmentation. These high molecular weight polymers that provide the pigmentation of the skin, hair, and eyes, have as main function the protection of the skin by absorbing potentially harmful UV radiation, minimizing the liberation of free - radicals in the basal layer.

Langerhans cells, the major antigen presenting cells in the skin, are dendritic cells that are created in the bone marrow, and migrate to and localize in the *stratum basale* region of the epidermis. When an antigen binds to the cell surface, they become active and migrate from the epidermis to the dermis and on to the regional lymph nodes. There, they sensitize T cells to generate an immune response and, in consequence of that, these types of cells are implicated in allergic dermatitis and also used as a target for the mediation of enhanced immune responses in skin.

Merkel cells are associated with the nerve endings and have as function cutaneous sensation, since they are concentrated in sensitive sites of the human body like the fingertips and lips. The major components of epidermis, the keratinocytes, are columnar and cuboidal, disposed in a single layer, are mitotically active, are connected to each other by desmosomes, and are attached to the basement membrane by hemi-desmosomes, in order to anchor the epidermis to the basement membrane.

Immediately above the *stratum basale*, there is the thickest layer of the epidermis with two to six rows of keratinocytes, with irregular morphology, connected by desmosomes, which form the *stratum spinosum*. In this *stratum*, keratinocytes have a larger cytoplasm, an amount of keratin filaments higher, numerous organelles, a more flattened shape and

lamellar bodies rich in lipids synthesized during the process of migration and differentiation of keratinocytes called Odland bodies.

The differentiation of keratinocytes continues in the following *stratum*, where the alleged precursors of the intercellular lipid lamellae of the stratum corneum, are arranged in parallel stacks containing lamellar subunits. The *stratum granulosum* has the last keratinocytes with nuclei that present keratohyalin granules and has a higher number and size of Odland bodies, filled with lipidic lamellar subunits and hydrolytic enzymes such as proteases, lipases, glycosidases. As these lamellar bodies approach the upper layers of the *stratum granulosum* and reach the interface between the *stratum* and the *stratum corneum*, they fuse with the cytoplasmatic membrane and extrude their content into the intercellular space. The secreted enzymes convert the glucosylceramides into ceramides, the lipids that form the dead layer of epidermis, and the short lamellar stacked disks reorganize to form the lamellar sheets that are observed in the *stratum corneum* intercellular space [3, 4].

The last layer before the main protective barrier of the skin is the *stratum lucidum*, which is only present in the palms of hands and soles of feet, where the skin is thicker. In this *stratum*, composed by three to five layers, cell nuclei and other organelles disintegrate, keratinization increases, and the cells become flattened and compacted. The structure of this layer is similar to the *stratum corneum*, with intracellular protein matrix and intercellular lipid lamellae.

1.1.2. Stratum Corneum: The Skin Barrier

The *stratum corneum*, the outermost layer, consists of 10 to 20 μm of high density and low hydration with only 10 to 15 cells in depth. This layer acts as primary barrier of the skin, regulating water loss from the body and preventing permeation of microorganisms and some harmful substances from the skin surface. The structure of *stratum corneum* is described as a brick and mortar structure, with corneocytes representing bricks in a matrix and intercellular lipids, with desmosomes, acting as molecular rivets between the corneocytes and the remain lipid within a cornified cell envelope. The corneocytes are elongated and flattened, lack a nucleus, are composed of about 70% to 80% keratin fibrils, which are cross-linked by intermolecular disulfide bridges, and have a protective function against physical and chemical injuries from the external environment. In the other hand, the intercellular lipid *lamellae* provide the barrier for water diffusion, thus preventing dehydration [1, 5].

The cornified cell envelope, with an approximate thickness of 15-20 nm, is a protein/lipid polymer structure formed just below the cytoplasmic membrane that subsequently resides on the exterior of the corneocytes. It consists in a protein envelope that contributes to the biomechanical properties of the cornified envelope and has a relevant role in the assembly of the intercellular lipid *lamellae*, due to cross-linking of structural proteins like involucrin, loricrin, cystatin A, filaggrin, a cysteine-rich protein and the 'small proline-rich' proteins. The other component of the cornified cell envelope is the lipid envelope, which has demonstrated to be essential for the formation of normal *stratum corneum* intercellular lipid *lamellae*, since in its absence the barrier function of the skin is disrupted, because the anchoring of the intercellular lipids, by covalent bounds, to the corneocyte protein envelope provides structure and barrier function of *stratum corneum*.

The lipid composition differs considerably from most other biological membranes, having longer and more saturated lipids and with the notable absence of phospholipids.

The major components of the lipid domains are composed by 50-60% long-chain ceramides, 20% cholesterol, 20%, free fatty acids, 10 to 20%, cholesterol esters, and 5% cholesterol sulfate. This specific composition of intercellular lipids and their structural arrangement in multiple lamellar layers within a continuous lipid domain is fundamental to the barrier function of the *stratum corneum*.

The ceramide structures are based on sphingolipids and have been classified based on their polarity (**Fig. 2**). The literature currently reports 12 CER subclasses that have been identified on the human skin, being ceramide I the least polar [6-9].

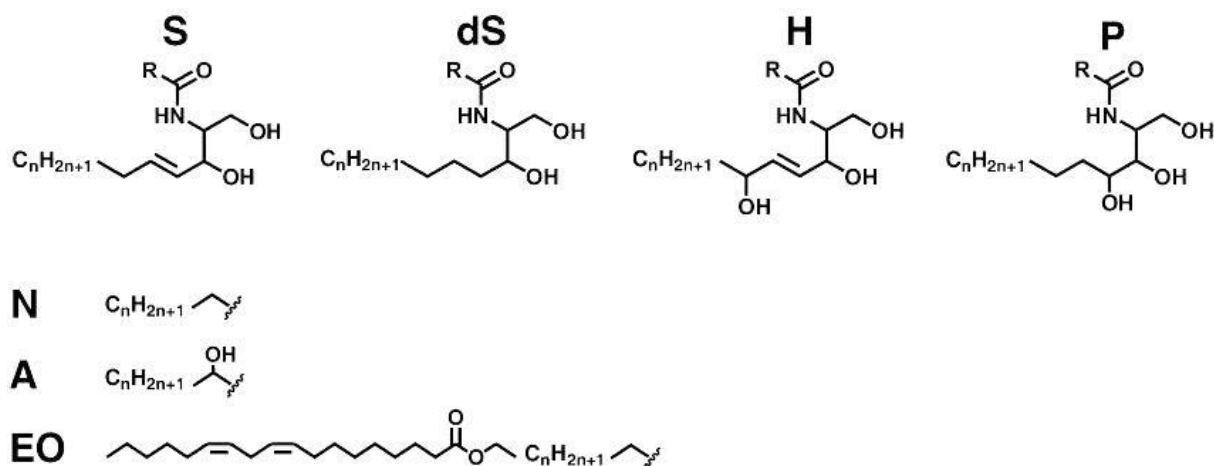


Fig. 2 Ceramides structure of the twelve ceramides present in the *stratum corneum* [7, 9]. Four possible sphingosine related chains (S, sphingosine; dS, dihydrosphingosine; H, 6-hydroxy-sphingosine; P, phyto-sphingosine) are linked via an amide bond to either of three different fatty acid components (N, non-hydroxy fatty acid; A, α-hydroxy fatty acid; EO, esterified ω-hydroxy fatty acid) resulting in, theoretically, 12 different CER subclasses. The literature has reported the presence of all but CER [1] in human SC. R represents one of the three different fatty acid chains.

Free fatty acids consist of a number of saturated long chain acids, varying in chain length between C16 and C36, with the most abundant being lignoceric acid (C24) and hexacosanoic acid (C26) and trace amounts of very long chain saturated and monounsaturated free fatty acids since C32 to C36.

The presence of cholesterol and cholesterol esters reduce the fluidity of the intercellular lipid *lamellae* and increase the fluidity of the extracellular lipid *lamellae*.

Besides being oriented parallel to the corneocytes cell wall and highly structured, the intercellular lipid *lamellae* exhibit heterogeneous phase behavior with multiple states of lipid organization. Through x-ray diffraction were identified two typical repeating units, a long lamellar structure or long periodicity phase (LPP) with a repeat length of ca. 134 Å and a short lamellar structure or short periodicity phase (SPP) with a repeat length of ca. 60 Å together with a fluid phase [7,10,11]. The LPP formation depends on the presence of long chain ceramides such as CER1, CER4, CER9 and the formation of the SPP is promoted by free fatty acids, which induce the transition from an hexagonal lateral sub-lattice to the predominant orthorhombic lateral sub-lattice and increase the fraction of SC lipids forming a liquid phase [7,12].

The organization of the intercellular SC lipids has been discussed and presented in different models. The domain mosaic model of the SC organization proposed by Forslind in 1993 (**Fig. 3**) [13,14] suggests that the lipids are organized in predominant crystalline/gel

domains surrounded by grain boundaries where the lipids are in a fluid crystalline state and form a continuous pathway.

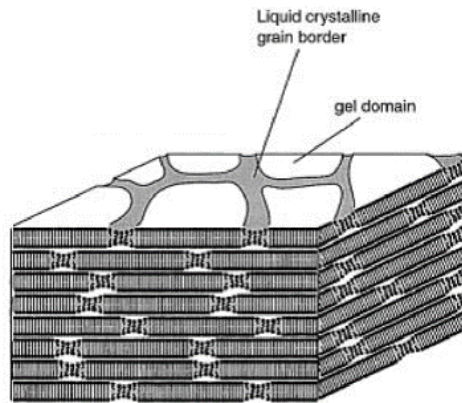


Fig. 3 Domain mosaic model of the SC organization proposed by Forslind [12].

Another model of the lipid matrix of stratum corneum, the sandwich model, focus on the molecular arrangements of the lipids [6,15] (**Fig. 4**). This model proposed by Bouwstra postulates the coexistence of crystalline and liquid crystalline lipid domains, describing complex structure of connected bilayers for the LPP where lipids are organized in 3 layers: two broad crystalline layers on the sides as most representative of lamellar phase and a narrow discontinuous fluid phase in the center, mainly composed by the fatty acid tail of the long chain ceramides CER1, CER4, CER9 and cholesterol.

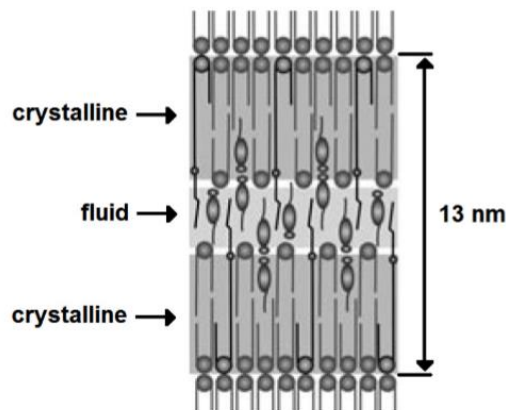


Fig. 4 The sandwich model of the SC organization proposed by Bouwstra [16].

The lattice spacing within these layers has been recognized as orthorhombic (crystalline), hexagonal (gel - like), and liquid lipid packing. These packing lattices correspond to the lowest, medium, and highest permeability levels, respectively. According to human stratum corneum, the orthorhombic lattice is the predominant, thus providing the major

contribution to the permeability barrier function, and toward the skin is observed an increased transition to the less tightly packed hexagonal lattice structure [7,17].

One of the latest models of the organization of lipid matrix of *stratum corneum* was proposed by Norlén and entitled the single gel phase model (**Fig. 5**) [12]. This model assumes an arrangement of lipids in the lower half of the SC in a coherent and single lamellar gel phase, without non-lamellar structures in continuous or bi-continuous arrangements like cubic, reversed hexagonal, reverse micelles or phase separation. In this gel phase model the hydrocarbon chains are packed simultaneously in a hexagonal and an orthorhombic order, thus allowing the prevailing of both phases.

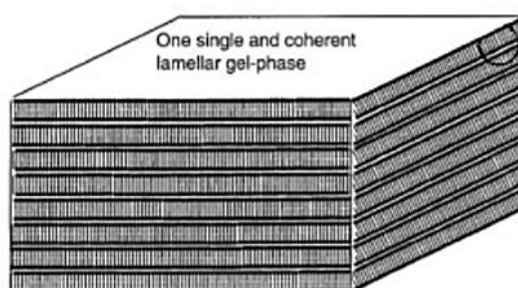


Fig. 5 Schematic representation of the single gel phase model of the SC organization proposed by Norlén [18].

The study of the lamellar and lipid matrix organization has a fundamental role since the unusual lamellar organization and composition of the intercellular lipids provide a very tight barrier to water diffusion. This phenomenon will influence the water content in SC and consequently affect the regulation of SC permeability.

The water content is about $30 \pm 5\%$ and also reflects the skin condition whereas it is a determinant factor to vital function of healthy skin by its relation to the mechanical properties, the enzymatic activity and the physical appearance of the SC [19,20].

Beside the lipid composition and organization, this property it's also correlated with the corneocytes and the Natural Moisturizing Factor (NMF). At a high level of hydration the corneocytes take up the water and tend to swell without affecting the mobility of solid components as keratin filaments, thus increasing the skin permeability [6,21]. On the other hand, the NMF, a mixture of hygroscopic, low molecular weight molecules, resulting by a degradation of filaggrin inside the corneocytes is responsible of maintaining adequate moisture levels in the stratum corneum, where NMF also function as humectant and plasticizer, binding water to aid swelling of the corneocytes.

The hygroscopic components of NMF such as lactic acid, urea, citrate and sugars contribute to a high osmotic strength that has the ability to retain water [7,22].

Due to the exceptional organization and composition of the SC, both by lipids and water content, the SC provides a great barrier function against hydrophilic compounds and in turn the viable epidermis is most restrain to highly lipophilic compounds. In other words, a hydrophilic substance won't easily penetrate the skin because it cannot enter the hydrophobic SC layer. A hydrophobic substance will enter the SC but it will remain stored inside since the next layer is hydrophilic.

1.1.3. The Dermis

The principal function of the dermis is to sustain and support the epidermis. It is a complex structure of dense irregular connective tissue, ca. 0.1-0.5 cm thick, composed by 2 layers, one more superficial, the papillary dermis and other in deeper tissue the reticular dermis. The papillary dermis is thinner, consisting of loose connective tissue containing elastic fibers, reticular fibers, capillaries and some collagen. The reticular dermis is formed by a thicker layer of dense connective tissue containing large blood vessels, elastic fibers, and tightly cross-linked collagen fibers arranged in layers parallel to the surface. The elastic and collagen fibers are produced and secreted by fibroblasts and have an enormous functional role by resisting deformational forces and returning the skin to its resting shape. The reticular layer also contains mast cells and macrophages involved in immune and inflammatory response, nerve endings, an extensive lymphatic network, and a number of appendages contained or originate within the dermis including hair follicles, sebaceous glands, and sweat glands. To surround the components of the dermis there is a gel-like ground substance composed of muco-polysaccharides, chondroitin sulfates, and glycoproteins [1,7].

Due to this structure, the dermis is easily permeated by most drugs, but may reduce the permeation to deeper tissues of very lipophilic drugs.

1.1.4. Skin Appendages

There are three appendages that are originated in the dermis: the hair follicles, sebaceous glands and sweat glands. The hair follicles are present at a fractional area of about 1/1000 of the skin surface, with the exception of the lips, palms of the hands, and soles of the feet. They have a sebaceous gland associated with each other that produces sebum, which lubricates and protects the skin, maintaining the skin surface at pH of about 5 [23]. The sebaceous glands are composed by free fatty acids, triglycerides, and waxes and are largest and most concentrated in the face and scalp where there are sites of origin the acne.

The erector *pilorum* muscle attaches the hair follicle to the dermis and allows the hair to respond to cold and fear.

The last appendages originated in the dermis are the sweat glands. These glands are present at a fractional area of about 1 in 10,000 of the skin surface and are located in most of the body with the exception of the lips and genitalia. They secrete sweat, a hypotonic salt solution with a pH approximate of 5 in response to emotional stress and body overheat, due to exercise or high environmental temperature [23].

Additionally to these, the nails are also considered as skin appendage, being the larger ones and consisting of both epithelial and connective tissue components. The matrix epithelium is responsible for the production of the nail plate whereas the nail bed epithelium mediates firm attachment [23,24]. The nails have essentially protective functions.

1.1.5. The Hypodermis

The hypodermis also none as subcutaneous tissue is the deepest and thickest layer of the skin. It is essentially composed of adipocytes, which are specialized in accumulating and storing energy in the form of fat, fibroblasts and macrophages. The adipocytes are arranged as lobules separated by connective tissue collagen and elastin fibers.

This layer has as main functions connect the dermis to the underlying muscles or bones, due to the connective tissue, heat insulation, protection against physical shock and also conduct the blood vessels and nerves through the skin [23].

1.2. Skin Drug Delivery

To treat various diseases and disorders, drugs can be administered into the body from different routes of administration. Although oral route is preferred for most patients it presents some disadvantages such as first-pass metabolism, irritation to gastric mucosa, which can cause nausea and vomiting, and destruction of drugs by gastric acid and digestive juices. To avoid these effects, innumerable compounds have been studied for thousands of years to be applied to the skin, thus making skin one route of drug delivery and also to enhance beauty as a cosmetics purpose.

The application, in a formulation, of pharmaceutical active ingredients on the skin can have a local or regional action, designated as topical delivery, or can pass through the skin into the bloodstream or lymph system and develop a systemic action at the target site, in a transdermal delivery.

Additionally, to overcoming first-pass metabolism and the adverse gastrointestinal environment, transdermal delivery offers significant advantages such maintenance and control of constant drug levels in the blood, which consequently will reduce the systemic side effects, or even eliminate them. This is very useful, especially, for drugs with a narrow therapeutic window or with a short half-live. Furthermore, this type of administration increases the patient compliance due to simpler dosage regimens and also because in case of adverse drug reactions, the treatment is easily interrupted by removing the formulation from the skin.

Due to all the advantages mentioned, topical and transdermal delivery constitutes a convenient, non-invasive and painless administration route, but in another hand have also some disadvantages [23,25].

The principal limitations of this route are the insufficient permeability that provides low effective therapeutic levels that often cannot be achieved, due to the outermost layer of the skin, the stratum corneum.

Other limitation that may produce different biological responses is the intra and inter-variability in the skin permeability between different subjects [23, 26].

To overcome these limitations it is possible to, in a healthy person, remove the *stratum corneum* by tape stripping to provide significantly increased permeability.

Since the percutaneous absorption of drugs for local or systemic delivery can be a desirable process it is fundamental to comprise the mechanisms by which the drugs and other substances penetrate the skin and how the skin permeation can be controlled. Thereby as the majority applications involve permeation to deeper tissues but other

applications may necessitate targeting the skin surface or appendages, it is relevant to highlight the importance of studying skin permeation pathways within the context of therapeutically active sites.

1.2.1. Routes of Penetration

To be successful a formulation when applied on the skin must allow the drug partition since the lipophilic SC to the systemic circulation passing through viable epidermis and the dermis by a mechanism of passive diffusion [23].

The transport of drugs through the skin has three potential pathways across the epidermis: through sweat ducts, via hair follicles and associated sebaceous glands, entitled transappendageal route, or across the intact *stratum corneum*, also known as transepidermal route. This route can be subdivided in transcellular, when the drug goes through the corneocytes and intercellular route when it goes between the corneocytes (**Fig. 6**) [6,23, 27,28].

Although these pathways are not mutually exclusive, since it is possible to a drug combine more than one penetration route, which will be dependent on its physicochemical properties.

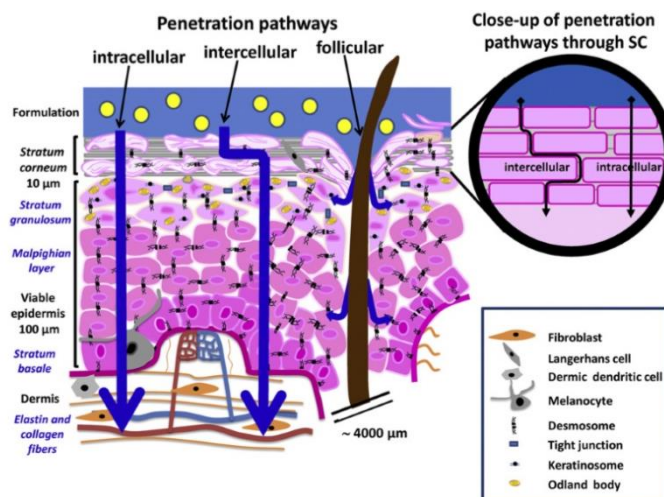


Fig. 6 Sketch of the three penetration pathways: intracellular, intercellular and follicular [28].

The appendage route has been considered as low resistance shunts, since the sweat glands and the hair follicles represent only 0.1% to 1% of the total skin surface area, comprising areas with less pilosebaceous units per area of skin and areas where the density of pilosebaceous units is higher such as the face and the scalp [6,23,29].

However, the interest in targeting the skin appendages, in particular the follicular delivery, has never been excluded because these follicles directly conduct to an epithelial membrane more permeable than the SC [29] and also because it facilitates the entry of large polar molecules and ions that are difficult to diffuse across the SC. For these reasons many delivery systems such as liposomes, nanoparticles and colloidal particles have been developed as formulation approaches.

On the other hand, the drug diffusion through the transcellular route implies a repeated partitioning of the molecule between the hydrophilic corneocytes, due to the hydration of their intracellular keratin matrix, and the lipophilic intercellular matrix surrounding them.

Although the intercellular route involves the intercellular lipid lamellae with the diffusion of molecules through the continuous and tortuous pathway, it provides the only continuous route through the SC and it is accepted by most scientists as the main pathway for most of the chemicals [7,23].

So any chemical that penetrates the skin will diffuse through the path of least resistance, which is also dependent on both the physicochemical properties of the drug and the skin condition at the time [7].

1.3. Factors Affecting Skin Permeation

The complex process of drug absorption from a topical or transdermal system starts with the release of the permeant from the dosage form, followed by diffusion into and through the *stratum corneum*, then partitioning to the more aqueous epidermal environment of viable epidermis and finally diffusion to deeper tissues or uptake into the capillaries in the dermis to the respectively cutaneous circulation. All of these steps are strongly dependent on the solubility and diffusivity of the permeant within each environment [6].

The relative solubility is a determinant factor in the release of the permeant from the dosage form vehicle and uptake into the lipophilic corneum layer and, therefore, the vehicle partition coefficient. On the other hand, the speed or diffusion coefficient at which the permeant moves within each environment is dependent on the permeant properties including physicochemical properties of the drug, physicochemical properties of the vehicle, skin condition and physiological factors and also application conditions.

Thereby, even though the thickness of the *stratum corneum* is only around 10 to 15 μm the intercellular route is highly tortuous and may be in excess of 150 μm . Since the

intercellular pathway is predominant, factors that influence movement into and within this environment are of greatest importance.

Despite of low homogeneity of the skin barrier, the steady-state permeation or also known as flux (J) of a drug through the SC can be simplistically described by Fick's first law of diffusion [1,6,23]:

$$J = \frac{dQ}{dt} = \frac{D \cdot K \cdot C_v}{h}$$

Where Q is the cumulative amount of drug permeated per unit of skin area, D is the drug diffusion coefficient in the SC, K is the partition coefficient of the drug between the formulation and the *stratum corneum*, C_v is the drug concentration in the vehicle, h is the drug diffusion path length.

1.3.1. Physicochemical Properties of the Drug

Knowing that there are many routes of drug administration and consequently different types of absorptions, it is relevant to highlight the ideal properties for the percutaneous absorption since the molecules that easily permeate through the skin are small and have a moderate lipophilicity [7]. Therefore it is important to know if the chemical structure of the drug is in agreement with the Lipinski's rules of five.

According with the first rule, the molecular weight of molecules should be low, less than 500 Da, in order to have higher diffusion coefficient (D) in the *stratum corneum*, since molecules with hydrogen bonding groups tend to diffuse slowly due to their ability to interact with the polar head groups of the intercellular SC lipids [1,30,31].

Additionally, the solubility of the molecule has also a high influence in its capacity to penetrate a membrane and it is correlated with the melting point, since when the melting point is inferior to 200°C, the drug has a good solubility in the intercellular SC lipid domain. [6]. The concentration gradient influences the drug flux within the skin and is mainly determined by the partition coefficient (K) of the drug.

The second relates the logarithm of the octanol-water partition coefficient (log P) with the partition behavior of the drugs within the skin [1,6,7], establishing that the log P should be lower than 5. In fact, a good partition behavior is associated to molecules with log P ranging from 1-3, since they have a good solubility in the lipophilic stratum corneum and also in the hydrophilic and water-rich viable epidermis [30,31]. If a drug is too lipophilic it

will partition to the SC easily but it will be retained there, in the intercellular lipids, therefore limiting its skin permeation rate. On the contrary, if the drug is too hydrophilic, the partition to the SC will be small, due to its inability to partition from the vehicle to the SC [6,32].

Another relevant property that influences permeation is the ionization potential, as long as ionized species have a lower permeability coefficient than the unionized counterpart and although the log P of the former is lower, the ionized species may permeate the skin through the transappendageal route or may also form neutral compounds by ion pairs with ions present in the skin [6].

Along with these physicochemical properties of the drugs, the pharmacokinetic parameters are also very important when analyzing the drug candidates. They must be pharmacologically potent, due to the ideally delivery dose below 20 mg/day and also because of the amount of therapeutic dose that can enter the skin through a reasonable area is limited [32]. Although these drugs have or may have a poor oral bioavailability and short biological half-life, they cannot be irritant to the skin and neither stimulate an immune reaction in the skin [25,32].

So to sum up, the diffusion coefficient or speed at which the permeant moves within each environment is associated to the permeant properties, since it can be influenced by molecular size, solubility, melting point, ionization and also factors related to the environment such as its viscosity.

1.3.2. Physicochemical Properties of the Vehicle

The first interaction between the drug and the skin relies on the capacity of the drug partition between the vehicle and the skin [1]. The vehicle has an essential role, since it can influence drug release from the formulation, by modulating the vehicle and SC partition, change the barrier function, of the skin in order to increase the drug solubility in the SC [23]. The alteration of the barrier function promotes the interaction with the intercellular lipid *lamellae* and protein components, and also promotes an occlusive effect due to the raise of the SC hydration, which can be obtained through the incorporation of chemical enhancers in the formulation, and by controlling the degree of occlusion in the case of transdermal systems [6,7,23].

Other relevant effects that affect the molecules permeation through the skin include the rate of vehicle evaporation, dissolution kinetics, solvent flux through the SC and modification of the vehicle composition [7,23]. To take in account all of these conditions

vehicles that have a low affinity to the permeants and in which the drug is less soluble are preferred [23].

1.3.3. Physiological Factors and Skin Condition

It is known that many factors, such as age, hydration, pH, ethnicity, gender and some skin disorders, may influence the percutaneous permeation of drugs [23,33,34].

With time, the aging of the skin leads to structural and biophysical alterations as the growing size of corneocytes and due to that, they consequently become less adherent to each other, decreased levels of SC lipids specially ceramides, decrease of epidermal turnover, TEWL and blood flow, which is a reflection of the atrophy of the dermis which becomes relatively acellular and avascular [6,23,35,36].

All these alterations can modify the skin permeability and lead to reduction of the permeability of hydrophilic compounds in aged skin, as it was been demonstrated [23,37]. On the other hand, newborns have a significant reduced skin barrier function which may lead to an increased permeability [37].

The skin permeation varies according to the anatomical site due to different morphologic and functional characteristics such as skin thickness, lipid content, blood flow or density of the hair follicles [23,36,38]. With the presence of these regional differences the percutaneous absorption usually decrease in the following order: genitals, the most permeable, > head and neck > trunk > arms > legs the least permeable [36].

Although there are not clear differences in same body site of males or females in the same race, there are some differences in ethnic groups. The SC of black people have more cell layers and higher density which may justify the smaller permeability [36].

Another factor that has influence on drug permeation is the skin hydration. If there is an increase in the water content of the SC, there is a consequently increase in the permeation, since occlusion directly affects the existent amount of water in the skin by preventing Transepidermal Water Loss (TEWL) phenomena [23,39].

Higher temperatures can also improve the skin permeability once this can enhance the fluidity of the intercellular lipids, by thermoregulation mechanisms alter the blood perfusion and increase drug solubility [23,40].

Lastly, the state of the skin also affects the skin permeation. If there are skin disorders such as eczema, psoriasis or acne, the barrier function will be compromised and hence the skin permeation will be increased [6,41].

So when developing a topical or transdermal system, all these factors must be taken in account, in order to achieve a desirable rate of drug delivery.

1.4. Dosage Forms Applied to the Skin

Due to disadvantages of oral administration, topical dosage forms have been developed and grouped as liquids, solids and semisolids, with special interest in the latter.

The semisolid dosage forms are traditionally used to treat topical diseases, being applied for ophthalmic, nasal, buccal, rectal or vaginal disorders, acting mostly as antibacterials, antifungals, anti-inflammatories and analgesics. These formulations must be cosmetically attractive but must substantially demonstrate that they are therapeutically effective, generally drugs incorporated into these dosages form show their activity on the surface of tissues or penetrate into deeper layers to reach the site of action.

The topical administration of drugs has recently gained an importance because of several advantages. Firstly, it can avoid gastrointestinal drug absorption problems caused by gastrointestinal pH and enzymatic activity and also drug interaction with food and drinks. Secondly, it may avoid the first pass effect since the drug will not pass through the systemic circulation, followed by gastrointestinal absorption and may be used to substitute oral administration when that route is unsuitable. Other advantages closely related to the patient are associated with the fact that they are non-invasive, less greasy and can avoid adverse reactions, considering that they can be easily removed from the skin. Furthermore, this type of administration allows a reduction of doses as compare to oral dosage forms and is not expensive. For all these reasons, the topical administration of drugs has shown a better patient compliance than other administration routes.

From all the dosage forms the most commonly used are creams, ointments and gels which have gained prominence [5].

Gels, according to the USP, are semisolid systems consisting of dispersions made up of either small inorganic particles or large organic molecules surrounded and interpenetrated by liquid. They can consist in a two phase system when the gel mass contains small particles disposed in a network or in a single-phase gel. This type of gels consists on uniformly organic macromolecules distributed through a liquid without an evident separation between the dispersed macromolecule and liquid. [42,43].

Gels can be classified based on colloidal phases, nature of solvent used, physical nature and also on rheological properties. However, they are mainly classified according to the nature of solvent. They can be either classified as hydrogels, if they contain water as

their continuous liquid phase, like bentonite magma, gelatin, cellulose derivatives and poloxamer gel. Or they can be classified as organogels, if they contain a non-aqueous solvent on their continuous phase.

To hydrogels gain gel structure they have to be completely dissolved in water or be dispersed as fine colloidal particles, thus the organic gelling agents, as cellulose polymer derivatives, which are generally high molecular weight, form gel structure due to their swelling and chain entanglement properties. And the inorganic gelling agents or gums gain gel structure because of their viscosity increasing nature.

Another relevant factor to the final structure of the gel, is the gel point, which is the gel forming temperature. Generally, cellulose derivatives obtain gel structure at temperatures above 60°C, in contrast to natural gums which gelify at lower temperatures, around 30 °C.

The organogels are also called oleaginous gels, since they are prepared with water insoluble lipids, such as fatty acids or glycerol esters that swell in water. To these type of gels, it is important to know the structural properties of the lipid, quantity of water in the system and the solubility of the drug incorporated, because they easily influence the nature of the liquid crystalline phase [5].

Gelling agents are compounds with a high molecular weight that are obtained from natural sources such as gelatin, collagen, agar or guar gum or via synthetic pathways, where they can be semisynthetic polymers as cellulose derivatives or truly synthetic polymers such as carbomer, poloxamer, carbopol.

Ideally, the gelling agent should be safe, inert, should not react with other formulation components and should possess suitable anti-microbial properties to prevent from microbial attack. Also when included in the preparation, it should produce a reasonable solid-like nature during storage, in order to be broken easily when subjected to shear forces generated by shaking the bottle, squeezing the tube, or during topical application [42].

In this project the hydroxypropylmethyl cellulose (HPMC), cellulose derivative, was used as gelling agent, since the gel point of these polymer dispersions varies from 50 to 90°C, being stable over a wide pH range.

The quality control involves the assessment of different physicochemical parameters, such as measurement of pH, drug content, viscosity, mechanical properties like texture profile analysis and spreadability, *in vitro* release studies which will be discussed further [5, 42].

However, gel application can raise some compliance issues, sometimes associated to body movements or cloth attrition and staining. This imposes the need to develop more convenient and safe dosage forms as an alternative to gels.

Topical films offer considerable advantages over gels, ointments and creams, because there is no need to spread the formulation, which allow an easier and cleaner application, and provides a more accurate dosing, with a continuous uninterrupted flow of the drug to the site of action. Additionally, the topical films have gained a remarkable patient compliance, due to the avoidance of multiple applications per day.

1.5. Non-Steroidal Anti-Inflammatory Drugs

An anti-inflammatory drug is characterized by its ability to eliminate or reduce an inflammatory state. The process of inflammation is complex and has a sequential order of events which starts with vasodilation. When vasodilation occurs, it leads to an increase of vascular permeability and blood flow to the inflammation area, resulting in redness and heat. These events will lead to an overflow of platelets, plasma proteins and leukocytes, which will raise the production of more pro-inflammatory mediators, like bradykinin and histamine, and mediate the inflammatory response, with the production of growth factors which will repair the injured tissue.

Non-steroidal anti-inflammatory drugs (NSAIDs) are the most popular and most widely used drugs for the treatment of pain, inflammation, and have been the cornerstone of pain management in patients with osteoarthritis and other painful conditions [44].

The non-steroidal anti-inflammatory drugs are among the most commonly used drugs. In the United States an estimated 5% of all visits to a doctor are related to prescriptions of non-steroidal anti-inflammatory drugs, and in the United Kingdom (UK) these prescription are, annually, more than 17 million [45].

These drugs are Cyclooxygenase-2 (Cox-2) inhibitors, preventing the production of pro-inflammation mediators, specially inhibiting the prostaglandin synthesis responsible for inflammation [45].

The majority of NSAIDs is administered orally but is associated to adverse effects such as gastric, duodenal irritation, nausea, vomiting and diarrhea.

Therefore, the use of NSAIDs topically prevents dose related adverse effects of such as acute renal insufficiency and prostaglandin inhibition, but also include higher concentration at the desired site that blood levels, absence of gastric degradation and hepatic first pass effect and can also increase permeation of drugs through the stratum corneum [46].

For all these advantages, it is ideal to deliver NSAIDs by topically administration.

1.5.1. Ibuprofen

Ibuprofen is a non-steroidal anti-inflammatory drug (NSAID) and is one of the most commercialized propionic acid derivatives. It is used for pain relief, osteoarthritis, fever reduction and also to minimize acute or chronic pain associated with inflammation (**Fig. 7**).

Conventionally, when administered orally the ibuprofen requires dosing at least three times daily because of high first-pass metabolism and short elimination half-life of the drug. Since ibuprofen has side effects related to gastric irritation, the repeated drug use can increase these and contributes to gastric discomfort, nausea, vomiting.

1.5.1.1. Physical and chemical properties

Ibuprofen is a white powder, but can also be a colorless, crystalline stable solid with a light characteristic odor. Although it has a poor solubility in water, 25 mg/L, it is very soluble in most of the organic solvents, as methanol, acetone, ethylic and propylic alcohol (**Table I**) [38,39].

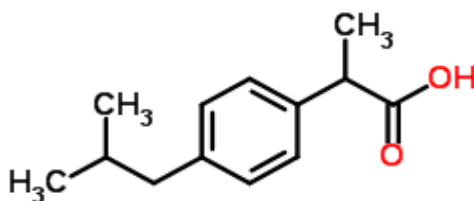


Fig. 7 Chemical structure of Ibuprofen [47].

Table I - Chemical properties of Ibuprofen [48].

Molecular Weight	206,28 g/mol
Molecular Formula	C ₁₃ H ₁₈ O ₂
Melting Point	75-78 °C
IUPAC name	2-[4-(2-methylpropyl)phenyl]propanoic acid
LogP	3,97

The ibuprofen is a good candidate for design into an effective topical or transdermal system, since it would, consequently, eliminate first pass metabolism, which would reflect an improvement in systemic bioavailability, ensure more uniform plasma levels, and reduce the

adverse effects already mentioned. Variables due to oral administration, such as pH, the presence of food or enzymes, would also be eliminated [46].

1.6 Aims of Dissertation

Delivery of drugs to/through the skin has been attractive as well as challenging area for research. However, the skin is an effective barrier to many compounds and these properties mean that only few topical/transdermal products have been developed, specifically to treat acute medical conditions, e.g. using non-steroidal anti-inflammatory drugs (NSAIDs) to provide a rapid treatment with short duration of action. This imposes the need for the development of new or improved ways of delivery NSAIDs in order to solve issues related to efficacy, dose, compliance, side effects or even bioavailability. Both transdermal and topical films remains a field largely unexplored.

Considering the advantages and limitations of topical and transdermal delivery, the purpose of this work consisted on:

- Developing and characterize the gel and films formulation for ibuprofen, as model drug, skin delivery;
- Evaluating the effect of different chemical enhancers on ibuprofen release and permeation behaviour;
- Assessing the impact of different polymers on *in vitro* adhesive properties;
- Understanding how composition variables and manufacture conditions impact drug product performance;
- Optimizing a topical formulation for paediatric population.

2. Pharmaceutical Development of Ibuprofen Hydrogels and Films for Skin Delivery

2.1. Introduction

Throughout the present work, pre-formulation, *in vitro* release and permeation studies were performed, along with the mechanical and adhesive properties evaluation to obtain an optimal formulation. The techniques and methods applied are described in the following sections.

2.2. Materials and methods

2.2.1. Materials

HPMC, Hydroxypropylmethyl cellulose, (Methocel[®] E4M) was a kindly gift from Colorcon[®] (Dartford, England), PEG 200 was obtained from Fluka, Chemie GmbH (Steinheim, Germany). PEG 300 was acquired from Scharlau (Sentmenat, Barcelona, Spain) and PEG 400 was purchased from Merck (Darmstadt, Germany). Ibuprofen was a gift from Medinfar (Amadora, Portugal), Propylene Glycol was obtained from José Manuel Gomes dos Santos, LDA (Odivelas, Portugal) and Isopropyl Alcohol was purchased from Sigma-Aldrich[®] (St. Louis, Missouri, USA). Eudragit[®] L 30 D-55 was provided from Evonik industries (Darmstadt, Germany) and Chitosan was a gift from Lusifar Químico Comercial (Lisboa, Portugal).

All other reagents or solvents were from analytical or from High Performance Liquid Chromatography (HPLC) grade.

2.2.2. Hydrogels Preparation and Characterization

Hydrogels were prepared with ibuprofen, 5% (w/w), water, isopropyl alcohol, propylene glycol and polyethylene glycol according to the composition presented in **Table 2**.

The HPMC (1,5%, w/w) was firstly dispersed in a volume of purified water and mixed under mechanical stirring at 25, 60 and 80°C.

The ibuprofen was previously dissolved in a mixture of co-solvents (**Table 2**) and then added to the HPMC solution under mechanical stirring, 400rpm, at the same temperature.

Hydrogels were stored for 24 hours at room temperature (approximately 25°C).



Fig. 8 Aspect of final gels obtained with the improvement of initial formulations.

Table 2 - Composition %(w/w) and coding for each hydrogel prepared in this work.

Formulation Code	Ibuprofen	HPMC	Propylene Glycol	PEG 400	Isopropyl Alcohol	Water
F ₁	5	1.5	20	-	-	73.5
F ₂	5	1.5	-	20	-	73.5
F ₃	5	1.5	20	20	-	53.5
F ₄	5	1.5	20	10	20	43.5
F ₅	5	1.5	10	20	20	43.5
F ₆	5	1.5	20	20	20	33.5

2.2.2.1. Mechanical Properties

Easy application and good retention at the site of application are two of the mechanical characteristics required for formulations which have been designed for topical application. To evaluate the hardness, compressibility, adhesiveness, cohesiveness, and elasticity of the hydrogels, a Texture Analyzer TA.XT Plus (Stable Micro Systems Ltd., Surrey, UK) was used.

Texture Profile Analysis (TPA) mode was carried out using an analytical probe (P/10, 10 mm Delrin) which was twice depressed into the sample at a defined rate (5 mm/s) to a desired depth (15 mm), allowing 15 sec of recovery period between the end of the first and the beginning of the second compressions. Cylindrical tubes with the same dimension were used to place the samples. Six replicates were performed at 25°C and 32°C, to simulate skin surface temperature, in the temperature controlled Peltier Cabinet for each formulation, providing the same conditions for each measurement [49].

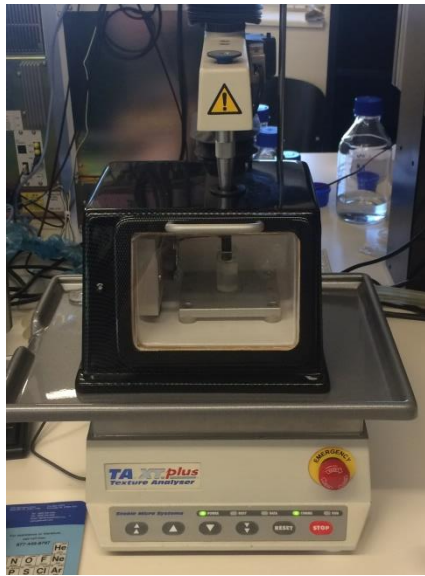


Fig. 9 TA.XT Plus Texture Analyzer with temperature controlled Peltier Cabinet and analytical probe P/10.

Data collection and calculation were performed using the Texture Exponent 3.0.5.0 software package of the instrument.

It was obtained a force–time curve, where the following mechanical parameters were determined [50]:

- Hardness: is given by the maximum peak force during the first compression cycle;
- Compressibility: is determined by the work required to deform the sample during the first compression and calculated from the area under the force–time curve I (AUC1);
- Adhesiveness: is the work required to overcome the attractive forces between the surface of the sample and the surface of the probe. This property is pointed as the negative force area for the first compression cycle and calculated from AUC2;
- Cohesiveness, is defined as the ratio of the area under the force– time curve produced on the second compression cycle and the area under the force-time curve of the first compression cycle, where both compressions are separated by a defined recovery period;
- Elasticity: results from the ratio of the time required to achieve maximum structural deformation on the second compression cycle to that on the first compression cycle.

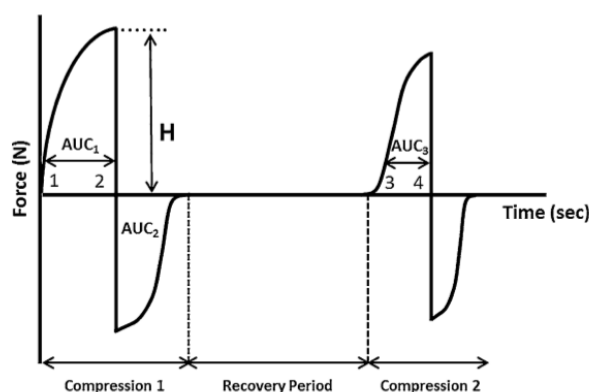


Fig. 10 Force-time curve obtained with texture profile analysis [51].

Where H stands for hardness, AUC1 to compressibility and AUC2 to adhesiveness. As mention before, the ratio between $AUC3/AUC1$ corresponds to the cohesiveness and the difference between time points 3:4/time points 1:2 establish the elasticity [51].

Additionally to TPA, a spreadability test was also performed with Texture Analyzer TA.XT Plus.

Spreadability is the easiness that a product can be spread. However, this property is also related to the firmness of the product, because the ease of spreading is often associated with a loss in firmness.

To perform the TTC Spreadability Rig the probe must be calibrated. Thus, the probe comes down and touches the bottom of the base cone, where the gel sample is placed an then return to a position precisely 25.0 mm over the flask cone. The test speeds is 3.0 mm/s and the evaluation consists on the penetration of the gel sample with the cone probe, to a depth of 2 mm above the sample holder surfaces. During penetration the force increases until the point of maximum penetration depth, which can be taken as the firmness value [52,53].

Thus, the gels spreadability indicates the extent of area to which gels readily spreads when applied to skin. This is a relevant factor, since the therapeutic potency of a formulation also depends upon its spreading value.

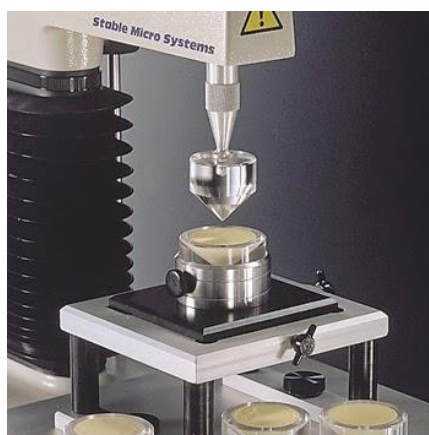


Fig. 11 Spreadability test apparatus, performed by Texture Analyzer TA.XT Plus.

In terms of time, spreadability is expressed in seconds and measures the time that a cone shaped probe takes to be separated from a conic recipient where the gel is loaded. The spreadability will be better when it takes less time to separate the probe from the base.

2.2.3. Films Preparation and Characterization

For the film preparation, different hydrogels were firstly obtained using the selected optimal conditions (**Section 2.2.2**). Briefly, a solution of HPMC (1.5%, w/w) was prepared under mechanical stirring at 80°C (see **Table 3**). Different polymers, Chitosan or Eudragit L30 D-55, were subsequently added to the HPMC solution (see **Table 4**).

Ibuprofen was dissolved in a mixture of co-solvents, composed of propylene glycol, isopropyl alcohol and different polyethylene glycols (PEG) 200, 300 or 400, according **Table 3**. This solution was added to the former and was further mixed under agitation of continuum mechanical stirring at 80°C.

Finally, to obtain the films, hydrogels were laminated using an Elcometer 3570 • 3580 Film Applicator, adjusted to 3 mm and dried for 24 hours at 37°C.

Table 3 - Hydrogel and film composition % (w/w) with co-solvent variation.

Formulation Code	Ibuprofen	HPMC	Propylene Glycol	PEG 200	PEG 300	PEG 400	Isopropyl Alcohol	Water
F ₆	5	15	20	-	-	20	20	33.5
F ₇	5	1.5	20	20	-	-	20	33.5
F ₈	5	1.5	20	-	20	-	20	33.5

Table 4 - Film composition % (w/w) with addition of adhesive agent.

Formulation Code	Ibuprofen	HPMC	Propylene Glycol	PEG 200	Isopropyl Alcohol	Water	Chitosan	Eudragit
F ₉	5	1.5	20	20	20	33.5	1	-
F ₁₀	5	1.5	20	20	20	33.5	-	1.5

2.2.3.1. Adhesive Properties

To evaluate the *in vitro* adhesive properties of the films, tack adhesion, tensile strength and elongation to break were performed with the Texture Analyzer TA.XT Plus (Stable Micro Systems Ltd., Surrey, UK).

The tack adhesion set up test (**Fig. 12**) consists of one stainless steel ball probe (P/IS), to ensure contact consistency with the adhesive, and a strip of double-sided tape, applied on the Peltier plate, to minimize the effect of facestock stiffness on the test data [43].

With measurements involving both mechanisms the adhesion and the separation between the probe and the sample we can obtain the following parameters:

- Adhesiveness: correspond to the typical mean maximum force. The height of the initial peak is related to the tack performance of the adhesive and this peak takes place at the point when the adhesive is first stretched;
- Elongation to detachment: measures the distance that the adhesive can be elongated before it detaches from the probe;
- Energy/work of adhesion: represents the area under the profile, which reflects the energy required to separate the adhesive from the probe.

Six replicates were carried out with data collection and calculation being performed using the Texture Exponent 3.0.5.0 software package of the instrument. The results are represented as mean \pm standard deviation (SD).



Fig. 12 Tack adhesion test with the stainless steel ball probe and double-sided tape applied on the Peltier plate.

2.2.3.2. Mechanical Properties

To perform tensile strength (TS) and elongation to break (EB %), the samples were cut into stripes with 73mm length and 37mm width and the TA.XTPlus Texture analyzer was equipped with a tension grip system.

The TS is calculated by dividing the maximum breaking force (N) by the cross sectional area (mm^2) of each film. Six replicates were taken on each sample in different places. Mean values and mean standard deviations were calculated for the film TS.

In turn, EB (%) is the ratio between the final length at the point of rupture and the initial length of the sample and is expressed in percentage [54].

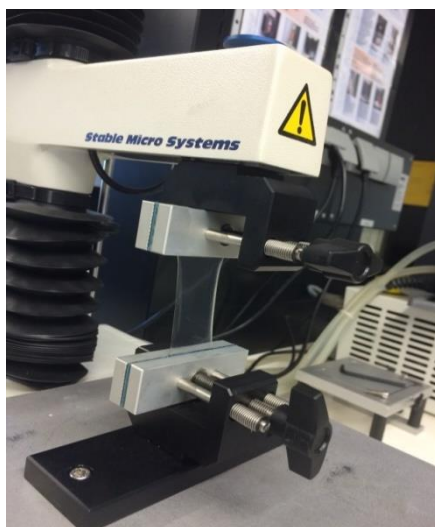


Fig. 13 TA.XTPlus Texture analyzer equipped with a tension grip system for the evaluation of the TS and EB (%) of the films.

2.2.4. *In vitro* release and Permeation Studies

According to The United States Pharmacopeial Convention (2009), performance test for topical drug products must be reproducible, reliable and able to measure drug release from the finished dosage form.

Although it is not a measure of bioavailability, the performance test must be capable of detecting changes in drug release characteristics from the finished [55]. In order to measure the drug release from gels and films were used Franz Cells.

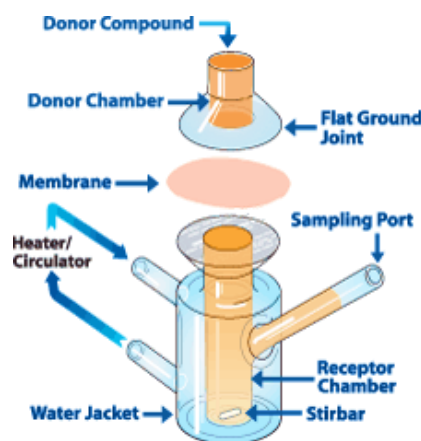


Fig. 14 Representative Franz Cell [56].

The Franz cells assembly consists of a donor chamber and a receptor chamber separated by a membrane and held together by a clamp (**Fig. 15**). This membrane keeps the product and the receptor medium separated and can be synthetic as cellulose ester or nitrate or biological as rabbit, pig or even human skin.

The receptor chamber is filled with Phosphate Buffered Saline (PBS) to mimic physiological conditions and the diffusion cells are thermo-regulated with a water jacket at 37°C.

The diffusion of the drug from the semisolid product across the membrane is monitored by sequentially collected samples of the receptor medium, at predetermined time points. After removing each aliquot the receptor compartment is made up with fresh medium and the drug content analysis, is usually determined by HPLC.

2.2.4.1. *In vitro* Release Studies

The release studies were performed with Franz cells (PermeGear, Inc., PA, USA) with a diffusion area of 0.636 cm² and a receptor compartment of 5 mL, which was filled in with PBS (pH=7.4) to guarantee the sink conditions. A dialysis cellulose membrane (MWCO~12,000, avg. flat width 33 mm, D9652, Sigma-Aldrich), as artificial membrane, was placed between both compartments that were thermo-regulated at 37 ± 0.5°C with a water pump, which circulated water through each chamber jacket. The receptor medium was stirred at 600 rpm.

The hydrogel or film samples were applied to the donor compartment and occluded with Parafilm® to prevent evaporation. Ozonol was used as commercial reference for comparison purposes. The assay was carried out 24 hour and at 8 predetermined time points were collected aliquots of 300 µL of the receptor compartment were collected and replaced with fresh medium.

All drugs were determined using the HPLC method described below.

2.2.4.2. *In vitro* Permeation Studies

The *in vitro* permeation studies were performed in the same Franz cells conditions of the *in vitro* release studies, but instead of the dialysis cellulose membrane, was used newborn pig epidermis as skin model, with the stratum corneum side facing up.

The newborn pig, provided by a local slaughterhouse, was cut and the subcutaneous fat was sectioned off. To separate the epidermis from the underlying dermis was used the heat separation technique. This technique consists in the immersion of the entire skin in hot water, around 60°C, for one minute and gently, with the help of forceps pulled the epidermal layer. This layer separation is more appropriate for permeants that are poorly water soluble [1].

After cutting the epidermal stratum in pieces of 2.5 x 2.5 cm², they were wrapped with aluminum foil and stored at -20°C until used.

The barrier function of the skin was monitored by measuring the transepidermal water loss (TEWL) and only the pieces that after hydration were below 20 g/m²h were used.

2.2.5. HPLC Determination of Ibuprofen

The quantification of Ibuprofen was performed using a high-performance liquid chromatography (HPLC) method, by a Shimadzu LC-2010 CHT apparatus equipped with a quaternary pump, an auto-sampler unit a CTO-10AS oven and a SPD-M20A detector. The column used for the analysis was a Luna Phenyl-Hexyl, Phenomenex[®] (Torrance, USA). A RP18 (4.6 mm x 125 mm) Lichrospher[®] 100 analytical column (Merck KGaA, Germany) with a pre-column was employed for the analysis.

Mobile phase consisted of a 60:40 (v/v) mixture of acetonitrile: water adjusted to pH 2.7 with orthophosphoric acid with a flow rate 1.0 mL/min, an injection volume of 20 µL and detection at 221 nm at 30°C.

2.2.6. Determination of pH

As a quality control parameter, the pH of the relevant formulations was measured, using a digital pH meter Consort C3010 (Dias de Sousa, Portugal), previously calibrated using buffer solutions with pH of 4.00, 7.00 and 10.01.

2.2.7. Ibuprofen Assay in Hydrogels and Films

A pre-defined mass of hydrogel formulation was dissolved in 5 mL of mobile phase solution and kept under agitation overnight. The solutions were filtered (0.45 µm) and appropriate dilutions were done in order to measure the drug content with HPLC method, previously described. Ibuprofen was also extracted from Ozonol for comparison purpose, using the same procedure.

For quantification of IBU in films, a pre-defined area of the film was cut and suitably diluted in mobile phase and kept under orbital agitation until complete dispersion. The samples were filtered (0.45 µm) and drug quantified by HPLC.

2.2.8. Statistical Analysis

The significance of differences was evaluated using both the F test and student's t test at the significance level of 0.05. This analysis was performed using Microsoft Excel (Microsoft Corp., Redmond, WA, USA).

3. Results and Discussion

Before the experimental tests were conducted, preliminary formulation studies included the selection of the gelling agent and the initial amount of enhancers and co-solvents, described in future sections.

3.1. Pre-formulation Studies

In order to investigate which was the best formulation (**Table 2**) for the preparation of the hydrogels with HPMC as the gelling agent, a preliminary study was made.

This polymer was chosen since it is a cellulose derivative and when this is dissolved in water it can be used as a binding agent, thickener, film former and also stabilizer.

The HPMC concentration was based in the literature, since when the temperature increase there is a slower decrease of viscosity until the gelation temperature is reached and after this temperature point, there is a keen increase in viscosity. The gelation point is concentration dependent, tending to decrease at concentrations higher than 2% [57]. For this reason the 1.5% (w/w) was chosen.

The PEG 400, propylene glycol and isopropyl alcohol were established also based on the literature, due to their wide use in topical formulations. The PEG 400 is used generally as plasticizer and permeation enhancer since it is a stable hydrophilic substance that is nonirritant to the skin and easily removed from the skin by washing. In turn, propylene glycol is commonly used as a plasticizer in aqueous film-coating formulations, acting also as preservative and has permeation enhancer properties, demonstrating a better efficacy when the SC is not fully hydrated, than in non-occlusive conditions [58]. The isopropyl alcohol was added as solvent, to obtain a homogeneous dispersion of the Ibuprofen in the gel.

3.1.1. Texture Profile Analysis

In order to compare the formulations and the commercial reference Ozonol, focusing on characterization related to pharmaceutical application and product performance, mechanical properties were evaluated, using the TA.XT Plus Texture analyzer.

Through the TPA mode and the resulting compression graphs, values of compressibility, hardness, adhesiveness, elasticity, and cohesiveness can be extracted.

Although some formulations could not be evaluated regarding to the ease with which the hydrogel can be applied on the skin, the hardness of the commercial reference

obtained was higher than all the formulations tested. This high value reflects an increased resistance to product deformation in TPA, which is a consequence of a high viscosity [50].

Table 5 - Mechanical properties of the Ibuprofen hydrogels formulations extracted from the TPA mode.

Formulations	Hardness (g.sec)	Compressibility (g)	Adhesiveness (g.sec)	Cohesiveness	Elasticity
F _{1 A}	-	2.93 ± 0.54	-4.91 ± 4.90	0.69 ± 0.08	0.49 ± 0.09
F _{1 B}	0.02 ± 1.95	4.40 ± 0.63	-5.69 ± 5.11	0.90 ± 0.16*	0.75 ± 0.15
F _{1 C}	-	2.21 ± 0.42	-8.42 ± 4.07*	0.70 ± 0.18	0.40 ± 0.13
F _{2 A}	-	2.18 ± 0.46	-6.20 ± 4.82	0.72 ± 0.09	0.42 ± 0.10
F _{2 B}	-	2.70 ± 0.29	-5.26 ± 2.4	0.86 ± 0.18	0.48 ± 0.08
F _{2 C}	-	2.59 ± 0.66	-6.14 ± 4.59	0.82 ± 0.04	0.51 ± 0.12
F _{3 A}	4.42 ± 0.56	5.43 ± 0.62	-5.27 ± 1.88	0.90 ± 0.06	0.79 ± 0.09
F _{3 B}	1.72 ± 2.43	5.36 ± 0.28	-7.81 ± 5.73*	0.87 ± 0.14	0.77 ± 0.09
F _{3 C}	1.95 ± 2.75	3.95 ± 0.43	-8.20 ± 4.95*	0.99 ± 0.10*	0.72 ± 0.11
Ozonol	11.49 ± 0.36	16.05 ± 1.57	-19.45 ± 2.68	0.98 ± 0.06	5.25 ± 0.43

The F number stands for formulation mentioned above, prepared at A: 25°C, B: 60°C and C: 80°C. * p > 0.05 vs. Ozonol.

With the rise of temperature, hardness values were diminished, although being associated with a higher fluctuation. According to previous studies, the hardness values obtained in this work are acceptable for skin gel application [50,51].

The choice of candidate formulation requires a balance between the hardness and the compressibility values, which should be low to ensure that the prepared gel is easily removed from the container and is also easy to apply it to the skin. Besides low values of hardness and compressibility the formulation should have high values of adhesiveness, which guarantees a good retention in the skin, since it is the work required to overcome the attractive forces between the surface of the hydrogel and the surface of the probe. In turn, cohesiveness provides information on the structural reformation following hydrogel application and a higher value warrants complete structural recovery [59]. Although, the Ozonol value for adhesiveness is very superior to the formulations prepared, the results reflect an easier application and a lower adhesion, but the latter is sufficient to keep the formulation in contact with the skin.

The last parameter evaluated with TPA, elasticity, is defined as the rate at which the deformed hydrogel returns to its original condition after the removal of the deforming force.

It is shown that larger hydrogel elasticity result from lower quantitative values of elasticity [59,60].

The analysis of the present results indicates that the F_{3 C}, which includes the addition of PEG 400 and propylene glycol in the formulation prepared at 80°C, is the most suitable sample. Although the majority of results show significant differences between the parameters of the tested formulations and the Ozonol, F_{3 C} do not exhibit statistical differences in comparison to the reference. Besides that, like in Ozonol, this formulation combines appropriate hardness and compressibility properties with higher values of adhesion and cohesion. To complement the TPA analysis, the spreadability test was performed (**Table 6**) to measure the ease of which a product can be spread. In this test lower values of firmness and work of adhesion correspond to an easy spreading of the hydrogel.

Table 6 - Spreadability properties of the Ibuprofen hydrogels formulations extracted from the Spreadability mode.

Formulations	Firmness (kg)	Work of Shear (kg.sec)	Stickiness (kg)	Work of Adhesion (kg.sec)
F _{1 A}	0.488 ± 0.004	0.084 ± 0.004	-0.658 ± 0.001	-0.045 ± 0.001
F _{1 B}	0.720 ± 0.001	0.149 ± 0.006	-0.771 ± 0.002	-0.070 ± 0.001
F _{1 C}	0.716 ± 0.003	0.152 ± 0.001	-0.742 ± 0.011	-0.076 ± 0.001
F _{2 A}	0.780 ± 0.001	0.173 ± 0.008	-0.819 ± 0.002	-0.089 ± 0.001
F _{2 B}	0.769 ± 0.008	0.149 ± 0.008	-0.766 ± 0.006	-0.080 ± 0.002
F _{2 C}	0.795 ± 0.003	0.181 ± 0.006	-0.796 ± 0.001	-0.088 ± 0.002
F _{3 A}	0.772 ± 0.199	0.219 ± 0.008*	-0.944 ± 0.001	-0.114 ± 0.001*
F _{3 B}	0.668 ± 0.002	0.138 ± 0.003	-0.857 ± 0.018	-0.078 ± 0.001
F _{3 C}	1.160 ± 0.019*	0.237 ± 0.015*	-0.776 ± 0.013	-0.086 ± 0.001
Ozonol	1.186 ± 0.047	0.264 ± 0.027	-1.045 ± 0.019	-0.109 ± 0.002

The F number stands for formulation mentioned above, prepared at A: 25°C, B: 60°C and C: 80°C. The results are expressed as mean ± SD (n=6). * p > 0.05 vs. Ozonol.

As the TPA results, the F_{3 C} was the formulation most similar to the commercial reference, without demonstrating significant differences in firmness and work of shear. Despite of the firmness values, this hydrogel had a low value of stickiness, which consequently leads to less time to separate the probe from the base.

3.2. Optimization of the Formulations

According to the pre-formulations studies, analysis of mechanical properties and the spreadability tests, the $F_3 c$ was chosen as the best composition. In order to promote a better dispersion and homogeneity of the IBU the isopropyl alcohol was added (**Table 2**). Consequently, the macroscopic and organoleptic properties of the hydrogel were also improved.

The addition of isopropyl alcohol, as a co-solvent, leads to formulation of F_4 , F_5 and F_6 which vary in the enhancer % (w/w) as displayed in **Table 2**.

The improved formulations were also analyzed with the same mechanical techniques presented in **Table 7**.

Table 7- Mechanical properties of the improved formulations extracted from the TPA mode.

Formulations	Hardness (g)	Compressibility (g.sec)	Adhesiveness (g.sec)	Cohesiveness	Elasticity
F_4	5.33 ± 0.48	5.49 ± 0.52	-8.83 ± 1.39	1.03 ± 0.04*	0.61 ± 0.05
F_5	7.55 ± 0.60	8.74 ± 0.62	-7.20 ± 1.94	0.97 ± 0.03*	0.69 ± 0.01
F_6	5.40 ± 0.15	5.86 ± 0.19	-17.09 ± 1.27*	1.05 ± 0.08*	0.75 ± 0.07
Ozonol	11.49 ± 0.36	16.05 ± 1.57	-19.45 ± 2.68	0.98 ± 0.06	5.25 ± 0.43

The results are expressed as mean ± SD (n=6). * p > 0.05 vs. Ozonol.

The results obtained from mechanical properties show that F_6 had lower values of hardness and compressibility than F_5 and higher values, in all parameters, than F_4 . Although, it demonstrated higher values than the F_4 for hardness and compressibility, which may difficult the extraction of the hydrogel from the container, these are not statistically different. In addition, F_6 has higher adhesive and cohesiveness properties, the latter even higher than Ozonol. This higher value allows a complete structural recovery and a good retention of the formulation in the skin.

Despite of lower adhesive values, F_4 formulation reveals a good balance of mechanical parameters due to lower hardness and compressibility, which might be explained with the reduced of PEG 400 concentration % (w/w).

The same trend was observed in spreadability test, presented in **Table 8**. Despite of higher values of firmness and stickiness exhibited by F_6 , among the tested formulations, the acquired results did not show any significant difference. This test also revealed that although

F₄ has low values of firmness, a higher % (w/w) of PEG 400 in F₅ did not increase this parameter, on the contrary, achieved an even lower value.

Even though the results display a low value of work of adhesion for F₆, this property, generally, follows the same trend as the stickiness. As higher the stickiness, higher will be the force to remove the probe from the sample, which is translated in high values of work of adhesion.

Table 8 - Spreadability properties of the Ibuprofen hydrogels formulations extracted from the TA.TX Plus Texture Analyzer.

Formulations	Firmness (kg)	Work of Shear (kg.sec)	Stickiness (kg)	Work of Adhesion (kg.sec)
F ₄	0.319 ± 0.020	0.109 ± 0.006	- 0.173 ± 0.005	-0.040 ± 0.001
F ₅	0.246 ± 0.027	0.110 ± 0.014	-0.313 ± 0.039	-0.053 ± 0.006
F ₆	0.485 ± 0.042	0.083 ± 0.014	-0.387 ± 0.062	-0.030 ± 0,004
Ozonol	1.186 ± 0.047	0.264 ± 0.027	- 1.045 ± 0.019	-0.109 ± 0.002

The results are expressed as mean ± SD (n=6).

3.2.1. In Vitro Release Studies

The *in vitro* release studies were performed using static Franz diffusion cells with a dialysis cellulose membrane and the conditions mentioned in section 2.1.4.1. These studies imply the release of the drug from the dosage form in the absence of the biological barriers, giving a good indication of the *in vitro* profile of the drug. The release profiles obtained with 100 mg of the three formulations and the commercial reference are displayed in **Fig. 16**.

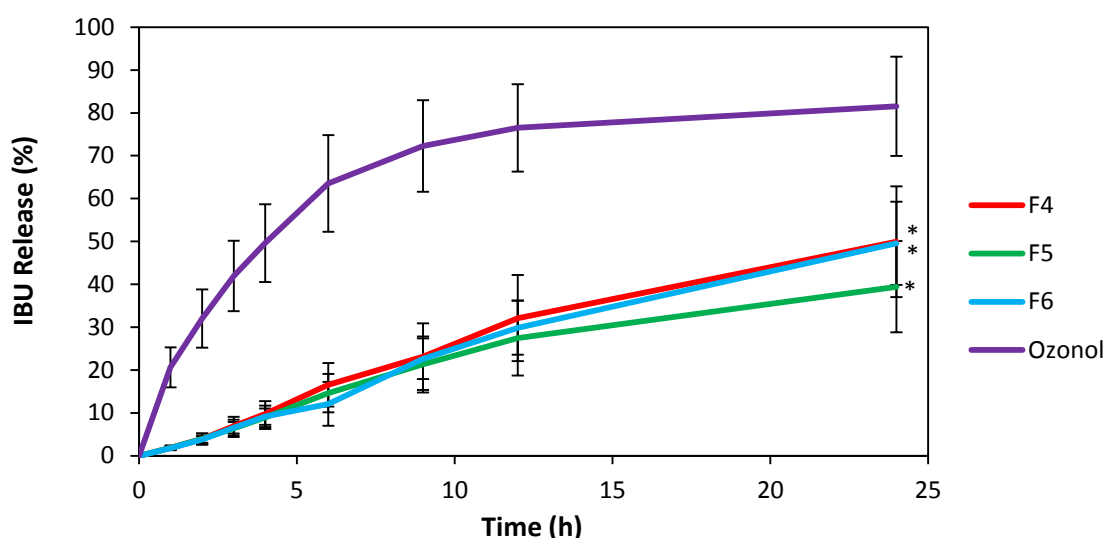


Fig. 15 *In vitro* release profiles of hydrogels formulations and the commercial reference Ozonol. A mass of 100 mg of each formulation was applied in the donor compartment. The results are expressed as mean ± SD (n=6). * p < 0.05 vs. Ozonol.

Marked differences in the release profiles were observed between the commercial reference, which demonstrated an approximated 60% of IBU being released within 6h, and the test formulations hydrogels, which had a much lower release around 15%. At the end of the 24 hours, 80% of IBU was released in Ozonol, contrastively to only 50% or less in tested formulations.

In agreement with mechanical properties, F₅, which had already shown higher values of hardness and compressibility and lower adhesiveness comparing to F₄ and F₆, was the worst formulation, with only 39% of drug release after the 24 hours. At the end of the study F₄ and F₆ reached 50% of IBU release, without any significant difference ($p > 0.05$).

Irrespective of the ratio of solvents employed, the release profiles were generally similar, being only observed small differences at 24 hours. Such behavior could be attributed to the higher solubility of the drug in PEG 400 [61].

Since F₄ and F₆ have both a higher ratio of PEG 400 (20%, w/w) the choice between these formulations was based on mechanical properties. As mention before, F₆ is harder and requires more strenght to be compressed than F₄, but on the other hand, it has higher values of adhesive and cohesiveness and for this reason F₆ was selected to proceed to the studies.

3.3. Effect of PEG Molecular Weight

The pre-formulation studies demonstrated a better performance for the formulation with same quantity of co-solvents (20:20:20 see **section 2.1.2**). However, to study the impact of chain length on hardness and compressibility of the hydrogels, PEGs with different molecular weight, 200, 300 and 400, were tested. The effect of this polymer chain change was also assessed in terms of permeation behavior.

3.3.1. Mechanical Properties

To evaluate the influence of the different PEGs, new hydrogels were prepared as indicated in **Table 3** and mechanical properties and spreadability were tested again. The results obtained are displayed in **Table 9**.

As it was expected, the hardness and compressibility decreased with the decrease of chain length of the PEG. Additionally, with this modification the adhesiveness values suffer a significate decrease comparing with the other samples, especially when PEG 200 was used, since only F₆ was not statistically different from Ozonol. The cohesiveness of F₆ and F₇ did

not evidence any significant difference between them and the commercial reference, with F₆ showing a better result in this parameter.

Table 9 - Mechanical properties of Ibuprofen hydrogels with PEG variation obtained from the TPA mode.

Formulations	Hardness (g)	Compressibility (g.sec)	Adhesiveness (g.sec)	Cohesiveness	Elasticity
F ₆	5.40 ± 0.15	5.86 ± 0.19	- 17.09 ± 1.27*	1.05 ± 0.08*	0.75±0.07
F ₇	4.00 ± 0.24	4.15 ± 0.28	-7.66 ± 2.83	0.97 ± 0.06*	0.64±0.09
F ₈	4.57 ± 1.93	5.31 ± 2.26	-11.75 ± 6.40	0.90 ± 0.21	0.69±0.21
Ozonol	11.49 ± 0.36	16.05 ± 1.57	-19.45 ± 2.68	0.98 ± 0.06	5.25±0.43

The results are expressed as mean ± SD (n=6). * p > 0.05 vs. Ozonol.

The spreadability test, presented in **Table 10** corroborates this prediction, with lower values of firmness, which allows a better spreadability with less amount of force required to perform the shearing process. Associated with a good spreadability are lower values of stickiness and consequently less force to remove the probe from the hydrogel, with lower results of work adhesion.

Table 10 - Spreadability properties of Ibuprofen hydrogels extracted from the TA.TX Texture Analyzer.

Formulations	Firmness (kg)	Work of Shear (kg.sec)	Stickiness (kg)	Work of Adhesion (kg.sec)
F ₆	0.485 ± 0.042	0.083 ± 0.014	-0.387 ± 0.062	-0.030 ± 0.004
F ₇	0.120 ± 0.025	0.021 ± 0.005	-0.144 ± 0.037	-0.011 ± 0.002
F ₈	0.201 ± 0.037	0.040 ± 0.007	-0.228 ± 0.043	-0.019 ± 0.003
Ozonol	1.186 ± 0.047	0.264 ± 0.027	- 1.045 ± 0.019	-0.109 ± 0.002

The results are expressed as mean ± SD (n=6).

The formulation containing PEG 200, F₇, exhibited lower values in all parameters, which indicate that, due to the low values of firmness and stickiness, this sample is the easier to spread. With significant differences between the variations of PEG and the Ozonol, the F₆ demonstrated the best spreadability properties, among the tested formulations, being the one with closest results from the reference.

3.3.2. *In Vitro* Release Studies

The same procedure (section 2.1.4.1) was followed, in order to assess the behavior of the formulations *in vitro* as it can be seen in Fig. 17. Using static Franz diffusion cells and a dialysis cellulose membrane, 150 mg of each formulation were placed in each cell to obtain an n=6.

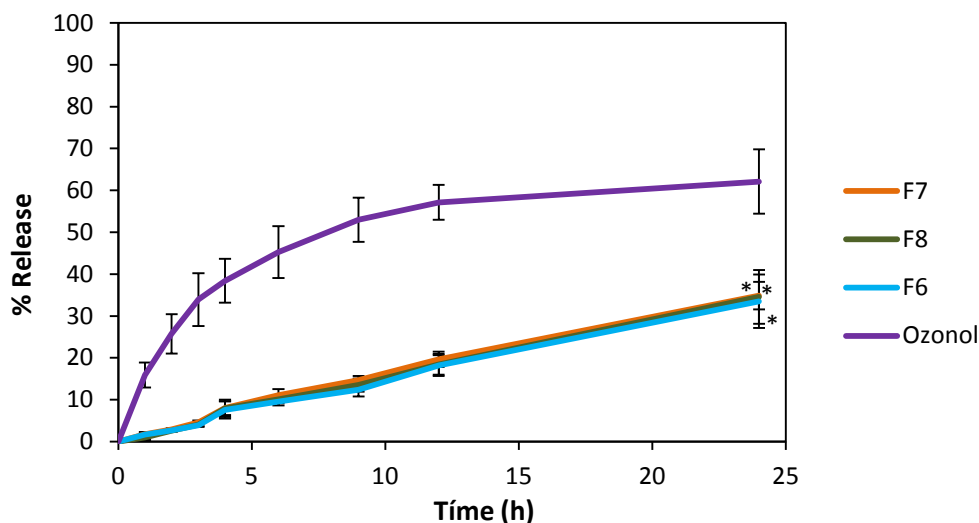


Fig. 16 *In vitro* release profiles of hydrogels formulations and the commercial reference Ozonol. A mass of 150 mg of each formulation was applied in the donor compartment. The results are expressed as mean \pm SD (n=6). * $p < 0.05$ vs. Ozonol.

The studies showed that the three tested formulations revealed very similar profiles, and a sustained release of ibuprofen is presented in comparison to Ozonol. Based only in these results it is not possible to choose the best gel formulation.

Despite of the changes in mechanical and spreadability properties, the PEGs variation, did not promote any significant differences ($p > 0.05$) between the formulations, which means that the molecular weight of PEG did not influence the ibuprofen release from the hydrogel.

It should be noted that a lower release of ibuprofen was observed for F₆ and Ozonol in comparison to the previous results (Fig 15), probably due to a higher hydrogel amount placed on the donor compartment that is not in direct contact with the dialysis membrane.

3.3.3. Determination of pH

The pH of formulations F₆, F₇ and F₈, F₉ and F₁₀, was measured using a digital pH meter Consort C3010 (Dias de Sousa, Portugal), previously calibrated. The results are presented in **Table II**.

Table II - Determination of hydrogels formulations pH.

Formulations	pH
F ₆	4.52
F ₇	4.52
F ₈	4.56
F ₉	4.77
F ₁₀	4.41

The values of pH were practically identical among the F₆, F₇ and F₈ formulations, being appropriate to topical use, since they are compatible with physiological skin conditions.

3.4. Effect on Pharmaceutical Dosage Form

The results of the hydrogel formulations in the release studies were lower than the results expected. To fight this problem we tried to transform the hydrogels in film systems using the hydrogel as the hydrophilic matrix with Elcometer 3570 • 3580 Film Applicator.

3.4.1. Preliminary Studies

Different thicknesses were tested in order to see which could achieve a better consistency and appearance after dried and also to see which thickness would be easier to remove from the backing layer without disrupting the film.

Thus, with these requests present, the films were adjusted to 3 mm and dried for 24 hours at 37°C to obtain what can be seen in **Fig. 17**.

Overall, the films prepared are thin, smooth and transparent, being slightly yellow when in presence of high content of chitosan.

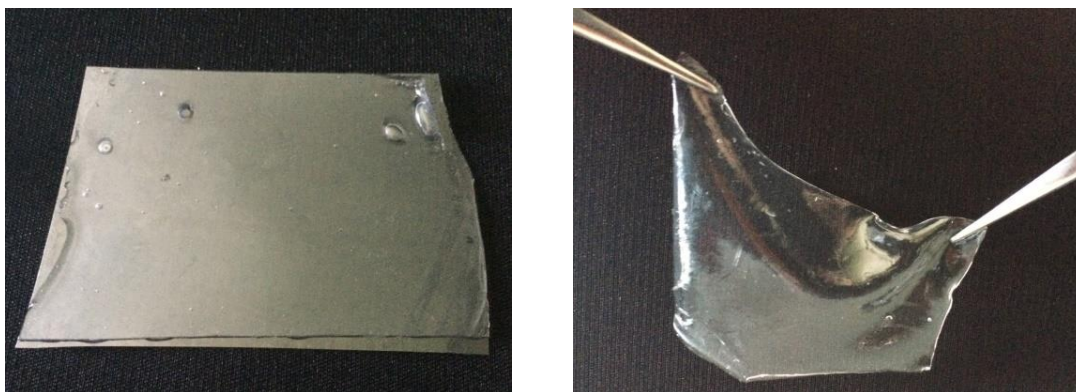


Fig.17 General aspect of films after drying, with and without backing layer respectively.

Samples with the composition presented in **Table 3** and in the film form, which exhibit content uniformity and acceptable aspect, were tested again.

3.4.2. *In vitro* Release Studies

The release behavior of ibuprofen from three different films containing PEG 200, PEG 300 and PEG 400, respectively, was assessed using the same conditions previously described in section **2.1.4.1**.

It can be observed that films provided a better performance in terms of release than the corresponding hydrogel formulations (**Fig. 18**). Such behavior might be explained by the close contact established between the films and the membrane, resulting from their best adhesion properties. Additionally, an inverse trend according to the PEG molecular weight is now observed F_{7p} and F_{8p} , with PEG 200 and 300 respectively, showed very similar release profiles, reaching both approximately 50 % after 24 hours, while for F_{6p} lower values (nearby 45 %) were obtained.

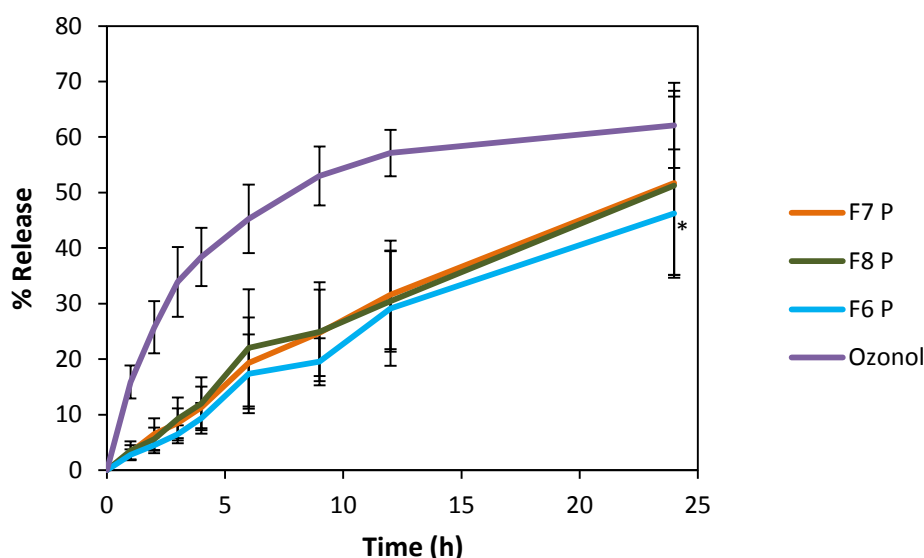


Fig. 18 *In vitro* release profiles of films formulations The results are expressed as mean \pm SD (n=6). * $p < 0.05$ vs Ozonol.

Such behavior could be attributed to the decreasing trend in the molecular weight of PEGs employed, since a lower weight is associated to a shorter chain length [62]. If the polymer chain is shorter, the entrapment of the drug could be diminished, therefore resulting in a higher release profile of ibuprofen.

Without showing any significant differences ($p > 0.05$), these premises support the use of patches as a better choice in terms of dosage form.

However, it can be observed that all the profiles still indicate smaller release values than the commercial reference.

3.4.3. *In vitro* Permeation Studies

Since the release profiles of films exhibited promising results, permeation studies were realized to see if the molecular weight of PEG influences on drug permeation. The PEGs and Propylene Glycol, both permeation enhancers, are usually incorporated in topical and transdermal patches, in order to modify the barrier properties of the SC and enhance the drug penetration and absorption, in the topical and transdermal systems respectively, across skin.

The results obtained are displayed in **Fig. 19** and the permeation parameters calculated from the obtained profiles are presented in **Table 12**.

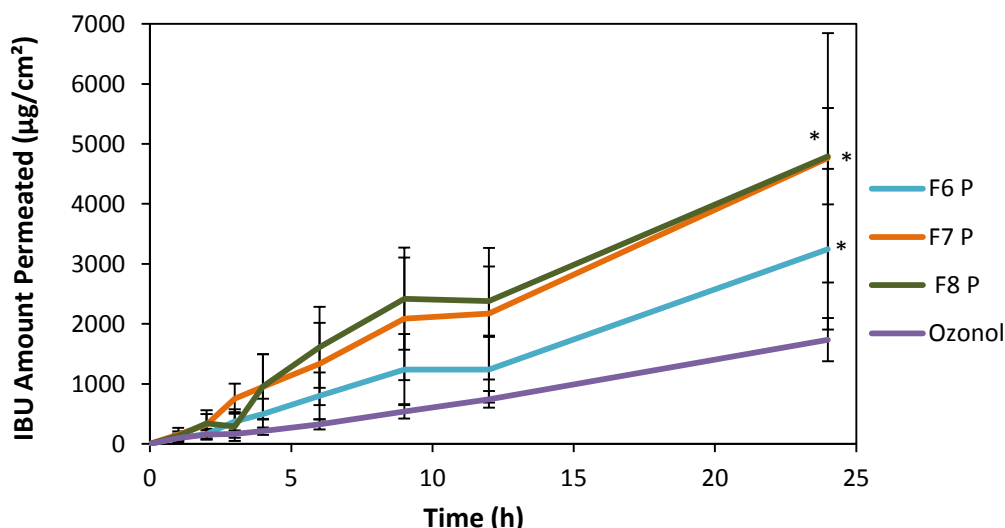


Fig. 19 *In vitro* permeation profiles of films formulations. The results are expressed as mean \pm SD (n=6) * p < 0.05 vs. Ozonol.

Although the F_{7 P} and F_{8 P} profiles demonstrated higher values of the IBU amount permeated than F_{6 P}, all formulations exhibited better permeation profiles than Ozonol, with statistically significant differences at the end of the 24 hours, (p<0.05). These results reinforce that of PEGs presenting lower molecular weight are associated with a shorter length of the PEG chains and consequently, the entrapment of the drug will be decreased leading to a higher release and permeation of ibuprofen.

Table 12 - Formulations and respective permeation parameters, according to *in vitro* permeation studies in epidermis.

Formulations	J _{ss} (µg/(cm ² hr))	K _p (cm/h)	Q ₂₄ (µg/cm ²)	Lag Time (h)
F6 P	148.185 \pm 86.577	0.011 \pm 0.006	3242.311 \pm 1467.119	0.254 \pm 1.565
F7 P	185.701 \pm 5.399	0.015 \pm 0.007	4766.077 \pm 2277.082	-
F8 P	185.641 \pm 54.896	0.017 \pm 0.009	5121.315 \pm 1135.147	-
Ozonol	122.439 \pm 31.369	0.010 \pm 0.002	1736.106 \pm 359.679	1.869 \pm 1.264

The J_{ss} represents the flux at steady-state; K_p the Permeability coefficient; Q₂₄ the Cumulative amount of IBU permeated after 24h. Data are expressed as mean \pm SD (n=6).

The decrease in PEG molecular weight had, in general, contributed to a higher flux, without a marked difference between F_{7 P} and F_{8 P}.

The three formulations exhibited better permeation parameters than the commercial reference as showed in the **Fig. 18**, which can be attributed to the presenting dosage forms, films vs. hydrogel (Ozonol).

The lag time was not considered a relevant parameter, since it is a back extrapolation of the x axis, and for F_{7p} and F_{8p} this extrapolation resulted in negative values.

Due to the best combined results in terms of release and permeation profiles, F_{7p} was selected to proceed to the studies.

3.5. The Effect of Adhesive

With the choice of F_{7p} some properties needed to be improved, namely the adhesiveness. To solve this problem some adhesives were added to the base composition and their influence upon adhesion was investigated.

3.5.1. Preliminary Studies

Based in the literature, some adhesives and different concentrations were tested until we obtain three candidates. The chitosan in a ratio of 1:5 of the HPMC (HPMC: Chitosan), and the Eudragit L30 D-55 in same proportion as HPMC, as it can be seen in **Table 4**.

The films prepared are thin, smooth and are distinguish in color, since the ones with chitosan have a slightly yellow appearance.

3.5.2. *In vitro* Release Studies

To assess how the implementation of an adhesive would influence the IBU release from the films, studies in the same conditions were performed according to section **2.1.4.1**, and the achieved results presented in **Fig. 20**.

Chitosan was used in a proportion of 1:5 HPMC: Chitosan and the Eudragit L30 D-55 was employed in same ratio of HPMC establishing a ratio of 1:1.

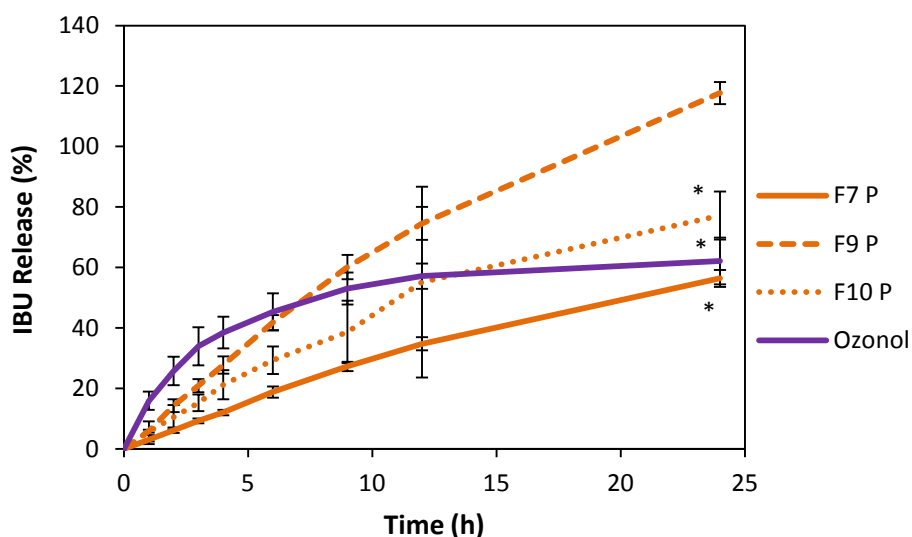


Fig. 20 *In vitro* release profiles of films formulations with different adhesives. The results are expressed as mean \pm SD (n=6).

From **Fig. 20** it can be observed that the inclusion of both chitosan and Eudragit enhance ibuprofen release, even exceeding the amount obtained with Ozonol formulation. Moreover, after 24 hours, all the formulations led to higher release extent of ibuprofen than F_{7 P}, which was the comparative film without adhesive.

The formulation with chitosan promoted the highest ibuprofen release percentage, being statistically different from all the formulations tested. This might be explained by an increased area of contact between the film and the dialysis membrane, since this formulation is the most adhesive.

Table 13 - Regression parameters resulting from the application of the different mathematical models to the experimental release data.

Function	Formulation	c1	c2	c3	R ²
Zero Order $c_1 \cdot t$	Ozonol	$7.625 \times 10^{-1} \pm 2.651 \times 10^{-2}$	-	-	0.9884
	F ₇ P	$1.858 \pm 5.351 \times 10^{-1}$	-	-	0.9892
	F ₉ P	$1.577 \pm 1.449 \times 10^{-2}$	-	-	0.9500
	F ₁₀ P	$2.124 \pm 1.160 \times 10^{-1}$	-	-	0.9621
First Order $c_1 (1 - \exp(-c_2 t))$	Ozonol	$3.640 \times 10^{-3} \pm 1.991 \times 10^{-5}$	$2.089 \times 10^{-4} \pm 1.145 \times 10^{-2}$	-	0.9883
	F ₇ P	$2.190 \times 10^{-2} \pm 1.918 \times 10^{-2}$	$9.246 \times 10^{-3} \pm 8.831 \times 10^{-3}$	-	0.9901
	F ₉ P	$3.802 \times 10^{-1} \pm 5.113$	$7.547 \times 10^{-2} \pm 1.748 \times 10^{-2}$	-	0.9757
	F ₁₀ P	$1.666 \times 10^{-2} \pm 1.712 \times 10^{-2}$	$1.459 \times 10^{-2} \pm 1.715 \times 10^{-2}$	-	0.9710
Higuchi $c_1 \cdot t^{0,5}$	Ozonol	$2.660 \pm 4.206 \times 10^{-1}$	-	-	0.8415
	F ₇ P	$6.703 \pm 7.893 \times 10^{-1}$	-	-	0.9099
	F ₉ P	$6.092 \pm 2.222 \times 10^{-1}$	-	-	0.9837
	F ₁₀ P	7.599 ± 1.043	-	-	0.8874
Weibull $c_1 (1 - \exp(-c_2 t^{c_3}))$	Ozonol	$9.156 \times 10^{-4} \pm 4.217 \times 10^{-2}$	$1.172 \pm 1.914 \times 10^{-1}$	$1.703 \times 10^3 \pm 9.023 \times 10^4$	0.9973
	F ₇ P	$3.244 \times 10^{-3} \pm 3.873 \times 10^{-2}$	$9.624 \times 10^{-1} \pm 2.463 \times 10^{-1}$	$5.313 \times 10^2 \pm 5.544 \times 10^3$	0.9904
	F ₉ P	$1.270 \times 10^{-4} \pm 5.428 \times 10^{-3}$	$6.204 \times 10^{-1} \pm 1.308 \times 10^{-1}$	$1.198 \times 10^3 \pm 3.049 \times 10^4$	0.9945
	F ₁₀ P	$8.479 \times 10^{-2} \pm 5.314 \times 10^{-3}$	$1.904 \pm 1.855 \times 10^{-1}$	$4.907 \times 10^1 \pm 2.144$	0.9962
Korsmeyer-Peppas $c_1 t^{c_2}$	Ozonol	$4.687 \times 10^{-1} \pm 5.614 \times 10^{-2}$	$1.170 \pm 4.043 \times 10^{-2}$	-	0.9973
	F ₇ P	$2.195 \pm 3.36418 \times 10^{-1}$	$9.412 \times 10^{-1} \pm 5.3518 \times 10^{-2}$	-	0.9905
	F ₉ P	$4.589 \pm 3.051 \times 10^{-1}$	$6.160 \times 10^{-1} \pm 2.516 \times 10^{-2}$	-	0.9946
	F ₁₀ P	$2.387 \pm 7.672 \times 10^{-1}$	$9.589 \times 10^{-1} \pm 1.119 \times 10^{-1}$	-	0.9645

The profiles obtained were fitted using different mathematical models in order to explain the mechanism of drug release [60]. The quality of fitting was assessed according to the value of coefficient of determination, the R², which should be as closest as possible or even one. The present results demonstrate best R² values for Weibull, following by Korsmeyer-Peppas and then the first order models. The fitting for Weibull allows characterizing dissolution profiles by the shape of the curve through c₃ parameter, which can be considered exponential if c₃ = 1, sigmoidal if c₃ > 1 or parabolic if the c₃ < 1 [63]. According to the achieved results, all formulations displayed a c₃ > 1, having for that a sigmoidal shape.

The prediction of the drug transport mechanism is made through the results obtained in Korsmeyer-Peppas with the c₂ values. If they are under, but close to 0.5, they

correspond to a Fickian diffusion process, on the contrary, if they are above, in the 0.5 and 1.0 range, they correspond to an anomalous (non-Fickian) transport, probably associated to polymer matrix relaxation. When the c_2 value is 1.0 a zero-order model is applied [64].

Thus, with this classification the results obtained were all above 0.5 but under 1.0, corresponding to a non-Fickian transport, where diffusion is attached with other mechanisms, with the exception of Ozonol, which, due to a value of 1.170 is associated to super case II transport. However, this semi-empirical model has a disadvantage, since it just considers the first 60% of the release.

The last fitting presenting a good R^2 values was the first-order model, where the c_1 parameter corresponds to the asymptotic value predicted for each profile. This parameter was higher for the F₉ P in comparison with all the formulations and the corresponding release rates were also larger, as extracted from the c_2 values, which are in agreement with the results obtained.

3.5.3. Mechanical and Adhesive Properties

The mechanical properties used to the characterized the films were the tensile strength (TS) and the elongation to break, which is expressed in percentage (EB %). Using the TA.TX Plus Texture Analyzer and the tensile grips (section 2.1.3.2) it is possible to evaluate the film properties in terms of their resistance to abrasion, with tensile strength, and flexibility assess with the elongation to break test. The results are expressed in **Table 14** along with the adhesive properties.

In vitro adhesion tests are used to characterize the adhesion of films being considered critical quality attributes. These tack tests assess the maximum force required to break a bond formed under pressure between the film and the steel probe. The adhesiveness was measured by "Transdermal Adhesive Tape", through tack test parameters, such as adhesiveness, energy of adhesion and distance to separation.

Table 14 - Mechanical and adhesive properties of different films with different adhesives.

Formulations	Elongation to break (%)	Tensile Strength (N/mm ²)	Adhesiveness (kg)	Distance to Separation (mm)	Energy of Adhesion (kg.sec)
F9 P	83.636	0.004136	0.008 ± 0.002	0.209 ± 0.136	1.364 ± 0.565
F10 P	54.458	0.004917	0.006 ± 0.001	0.021 ± 0.001	0.323 ± 0.002
F7 P	66.786	0.003354	0.008 ± 0.001	0.056 ± 0.025	0.553 ± 0.244

Results are expressed in Mean ± SD with n=6.

It is important that this type of dosage forms possess some characteristics such as enough flexibility to follow the movements of the skin and capacity to resist to the mechanical abrasion caused by clothes. To achieve that, a film should be hard, which is a reflex of a high TS, and should be tough demonstrating a high percentage of EB [65].

A higher value of elongation to break is demonstrated with higher flexibility properties of the film. This is proven with the results obtained, which show that the formulation F_{9 p} had more flexibility than the film without adhesive and the F_{10 p} formulation. The Eudragit L30 D-55 sample exhibited even lower values than the F_{7 p} but, on the other hand, had improved its TS value. Both adhesive formulations were significant differences with F_{7 p}, showing higher values in this parameter.

The results presented for tack adhesion showed that the adhesiveness was practically the same for all formulations, but in terms of energy of adhesion, the F_{9 p} required a stronger force to separate the probe from the adhesive film. Associated with a high value of energy of adhesion is a longer distance of separation, which is in agreement to results obtain.

Despite of a higher residue due to, higher distance to separation and consequently higher energy of adhesion, the F_{9 p} was chosen as the best adhesive tested formulation.

3.5.4. *In vitro* Permeation Studies

To assess the IBU amount permeated from films, including different adhesives another study was performed, taking the formulation without adhesive and the commercial one as references (**Fig 21**).

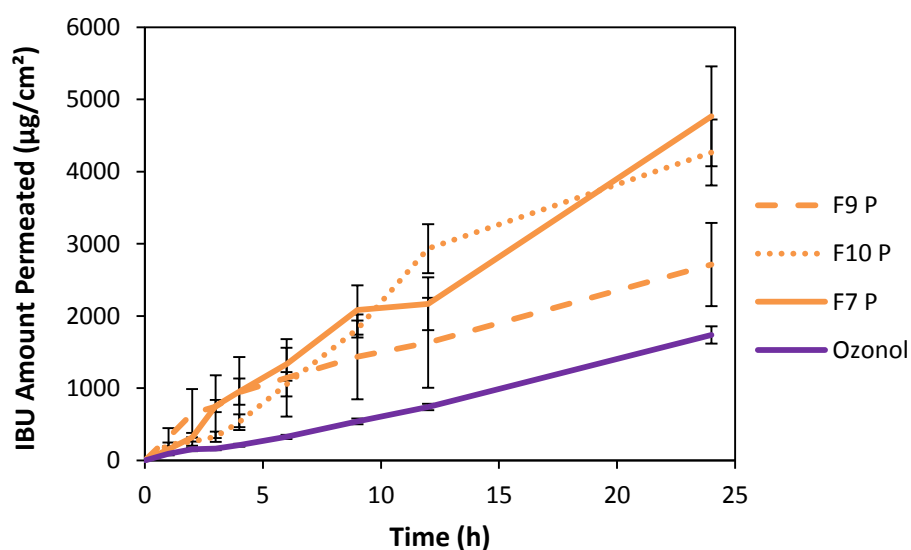


Fig. 21 *In vitro* permeation profiles of films formulations with the best adhesives. The results are expressed as mean \pm SEM (n=6).

Unexpectedly, the results achieved in the permeation studies, exhibited an inversion of the release profiles obtained in **Fig 20**. The F_{7p} , which promoted the lowest percentage of release correspond now to the higher permeation rate, followed by Eudragit containing formulation (F_{10p}) and finally chitosan based formulation. This trend could be ascribed to the chitosan film formation properties, already established for wound healing [66,67]. Despite of the bioadhesive properties of chitosan pointing to an increase in drug penetration, its film formation ability suggests that the drug is retained at the surface, not allowing it to permeate to deeper skin layers.

On the other hand the combination of HPMC with Eudragit has already been reported to promote increased drug permeation rates. As the study carried out by Irfani (2011) permeability coefficients follow the same trend as the one observed for fluxes (J_{ss}) [68].

Table 15 - *In vitro* permeation parameters for films with the presence of adhesives and Ozonol.

Formulations	J_{ss} ($\mu\text{g}/(\text{cm}^2\text{hr})$)	Kp (cm/h)	Q24 ($\mu\text{g}/\text{cm}^2$)	Lag Time (h)
F9 P	69.37 ± 61.58	0.009 ± 0.007	2714.290 ± 1730.763	-
F11 P	132.64 ± 110.230	0.010 ± 0.008	4265.539 ± 1368.988	-
F7 P	185.701 ± 5.399	0.015 ± 0.007	4766.077 ± 2277.082	-
Ozonol	122.439 ± 31.369	0.010 ± 0.002	1736.106 ± 359.679	1.869 ± 1.264

The results are expressed as mean ± SD (n=6).

After all the studies performed, the pH of these final formulations was measured, as displayed in **Table 11**. According to the previous measures, the pH obtained was compatible with physiological skin conditions.

Different theoretical mathematical models were used to estimate ibuprofen values of permeability coefficient, based on physicochemical properties of the drug such as molecular weight and coefficient partition (log P), [69] as it can be seen from **Table 16**.

Table 16 - Estimated Ibuprofen values of Kp (cm/h), from different permeation correlation equations.

Equations	Permeation Correlation	Kp (cm/h) estimated Ibuprofen
Potts and Guy	$\text{Log } k_p = 0.71 \log P - 0.0081 \text{MW} - 2.74$	0.026
Flynn and Amidon	$\text{Log } k_p = -1.44 + 0.79 \log P - 1.45 \log \text{MW}$	0.022
Wilschut et al. A	$\text{Log } k_p = -2.12 + 0.502 \log P - \log (14.0 + P^{0.5})$	0.009
Wilschut et al. C	$\text{Log } k_p = -1.55 + 0.481 \log P - 0.143 (\text{MW})^{0.5}$	0.020
Wilschut et al. D	$\text{Log } k_p = -1.55 + 0.481 \log P - 0.143 \sqrt{\text{MW}}$	0.020

Experimental values are in good agreement with predicted ones, highlighting that the strategy employed for the pharmaceutical development of the film based formulations, exhibit a better performance for skin drug delivery.

4. Concluding Remarks

The work presented in this dissertation, aimed at developing an optimal formulation for skin delivery of ibuprofen as model drug. From a technological point of view, hydrogels and films were sequentially assessed in terms of mechanical properties, release and permeation behavior, as critical quality attributes. The effect of composition variables and the production conditions on the different dosage forms were also inspected.

The hydrogel mechanical analysis and the respective release studies allowed to have an insight on the best base composition, stressing the need to control the balance between the hardness and compressibility with adhesiveness and cohesiveness properties, in order to promote an appropriate release from the container, but also, an easier application when the gel is spread on the skin.

In vitro release studies showed that, PEG 400 was a better co-solvent for ibuprofen than propylene glycol. The following screening to study the influence of molecular weight of PEG on release and permeation rate revealed an inverse correlation between this composition variable and the selected critical attributes, pointing PEG 200 as the best enhancer.

To improve the results obtained, the dosage form was changed to films and an increase of drug release was observed. However with this modification another issue emerged, since the films were lacking adhesion. A screening of adhesives was then made, revealing that HPMC: Chitosan, in a ratio 1:5, followed by and HPMC: Eudragit L30D-55 in a 1:1 proportion, % (w/w), provided the best adhesive properties and promoted an improvement of drug *in vitro* release and permeation. Several mathematical models were used to elucidate the release mechanisms from the different films. *In vitro* release kinetics was shown to be driven by diffusion coupled with polymer relaxation mechanisms.

Based on permeation profiles of ibuprofen and the mechanical parameters of films, it was concluded that different adhesives led to different permeation rates, HPMC: Eudragit L30D-55 (1:1) formulation exhibiting reaching a better performance than the commercial reference.

The main findings achieved in this work may provide a promising basis to further *in vivo* studies to support the formulation fine-tuning for a pediatric use.

5. Future Work

Based on the latter unexpectedly results, the follow up of this work would begin with the performance of other *in vitro* permeation studies, in order to clarify the results obtained.

Furthermore, although the chitosan film formation ability suggests that the drug is retained at the surface, it would be interesting to investigate the quantification of ibuprofen throughout skin including deeper layers, performing the permeation studies using the dermis and epidermis.

In order to have an insight about the behavior of the film *in vivo* and in its adhesive properties, the formulation could also be assessed through skin irritation test and through *in vivo* bioadhesive test, using the established guidelines on quality.

Since the overall results have showed a better performance than the commercial reference, they could provide a promising basis to minimize the lack of these products on the market.

6. References

1. A.E., B.H. and W.A. C., *Transdermal and Topical Drug Delivery*. 2012.
2. Skin layer image. Available from <http://theacneproject.com/what-causes-pimples> . Accessed on 4/06/2016.
3. MENON, G.K., New insights into skin structure: scratching the surface. *Advanced Drug Delivery Reviews*, 2002. **54**: p. S3-S17.
4. MARKS, R., The stratum corneum barrier: The final frontier. *Journal of Nutrition*, 2004. **134**(8): p. 2017S-2021S.
5. COX, Gad, and Shayne, eds. *Pharmaceutical Manufacturing Handbook: Production and Processes*. 2008, John Wiley & Sons. 267-311.
6. VITORINO, C., J. Sousa, and A. Pais, Overcoming the Skin Permeation Barrier: Challenges and Opportunities. *Current Pharmaceutical Design*, 2015. **21**(20): p. 2698-2712.
7. SILVA, C.S., *Skin Structure and Drug Permeation*. 2008.
8. TAMURA, E., A. Naoe, and T. Yamamoto, The roughness of lip skin is related to the ceramide profile in the stratum corneum 2016.
9. VAN SMEDEN, J., et al., LC/MS analysis of stratum corneum lipids: ceramide profiling and discovery. *Journal of Lipid Research*, 2011. **52**(6): p. 1211-1221.
10. BOUWSTRA, J.A., et al., The role of ceramide composition in the lipid organisation of the skin barrier. *Biochimica Et Biophysica Acta-Biomembranes*, 1999. **1419**(2): p. 127-136.
11. McINTOSH, T.J., M.E. Stewart, and D.T. Downing, X-ray diffraction analysis of isolated skin lipids: Reconstitution of intercellular lipid domains. *Biochemistry*, 1996. **35**(12): p. 3649-3653.
12. BOUWSTRA, J.A., et al., Phase behavior of lipid mixtures based on human ceramides: coexistence of crystalline and liquid phases. *Journal of Lipid Research*, 2001. **42**(11): p. 1759-1770.
13. FORSLIND, B., A DOMAIN MOSAIC MODEL OF THE SKIN BARRIER. *Acta Dermato-Venereologica*, 1994. **74**(1): p. 1-6.
14. FORSLIND, B., L. Norlen, and J. Engblom, A structural model for the human skin barrier. *Colloid Science of Lipids: New Paradigms for Self-Assembly in Science and Technology*, 1998. **108**: p. 40-46.
15. ELIAS, P.M., Stratum corneum defensive functions: An integrated view. *Journal of Investigative Dermatology*, 2005. **125**(2): p. 183-200.
16. Leiden University Repository access on 19-06-2016.
17. NORLÉN, L., A. Al-Amoudi, and J. Dubochet, A cryotransmission electron microscopy study of skin barrier formation. *Journal of Investigative Dermatology*, 2003. **120**(4): p. 555-560.

18. NORLÉN, L., Skin barrier structure and function: the single gel phase model. *J Invest Dermatol*, 2001. **117**(4): p. 830-6.
19. HARDING, C.R., et al., Dry skin, moisturization and corneodesmolysis. *International journal of cosmetic science*, 2000. **22**(1): p. 21-52.
20. JOHNSEN, G.K., O.G. Martinsen, and S. Grimnes, Estimation of in vivo water content of the stratum corneum from electrical measurements. *The open biomedical engineering journal*, 2009. **3**: p. 8-12.
21. ELIAS, P.M., The skin barrier as an innate immune element. *Seminars in Immunopathology*, 2007. **29**(1): p. 3-14.
22. ROBINSON, M., et al., Natural moisturizing factors (NMF) in the stratum corneum (SC). I. Effects of lipid extraction and soaking. *Journal of Cosmetic Science*, 2010. **61**(1): p. 13-22.
23. WAITERS, K.A. and K.R. Brain, Dermatological formulation and Transdermal systems. *Dermatological and Transdermal Formulations*, 2002. **119**: p. 319-399.
24. HANEKE, E., Anatomy, biology, physiology and basic pathology of the nail organ. *Hautarzt*, 2014. **65**(4): p. 282.
25. FINNIN, B.C. and T.M. Morgan, Transdermal penetration enhancers: Applications, limitations, and potential. *Journal of Pharmaceutical Sciences*, 1999. **88**(10): p. 955-958.
26. BROWN, M.B., et al., Dermal and transdermal drug delivery systems: Current and future prospects. *Drug Delivery*, 2006. **13**(3): p. 175-187.
27. BERRY, B.W., Novel mechanisms and devices to enable successful transdermal drug delivery. *European Journal of Pharmaceutical Sciences*, 2001. **14**(2): p. 101-114.
28. BOLZINGER, M.-A., et al., Penetration of drugs through skin, a complex rate-controlling membrane. *Current Opinion in Colloid & Interface Science*, 2012. **17**(3): p. 156-165.
29. OGISO, T., et al., Transfollicular drug delivery: Penetration of drugs through human scalp skin and comparison of penetration between scalp and abdominal skins in vitro. *Journal of Drug Targeting*, 2002. **10**(5): p. 369-378.
30. BOS, J.D. and M. Meinardi, The 500 Dalton rule for the skin penetration of chemical compounds and drugs. *Experimental Dermatology*, 2000. **9**(3): p. 165-169.
31. MAGNUSSON, B.M., et al., Molecular size as the main determinant of solute maximum flux across the skin. *Journal of Investigative Dermatology*, 2004. **122**(4): p. 993-999.
32. A. NAIK, Y.E.K., Transdermal drug delivery: overcoming the skin's barrier function. 2000 p. 318-326.
33. IDSON, B., *J. Pharm. sci.*, 1975. **64** p. 901-924.
34. WILLIAMS, A.C., *Trandermal and topical drug delivery; from theory to clinical practice*. 2003: London.

35. BATISSE, D., et al., Influence of age on the wrinkling capacities of skin. *Skin Research and Technology*, 2002. **8**(3): p. 148-154.
36. ROSKOS, K.V., H.I. Maibach, and R.H. Guy, The effect of aging on percutaneous-absorption in man. *Journal of Pharmacokinetics and Biopharmaceutics*, 1989. **17**(6): p. 617-630.
37. GIUSTI, F., et al., Skin barrier, hydration, and pH of the skin of infants under 2 years of age. *Pediatric Dermatology*, 2001. **18**(2): p. 93-96.
38. WILHEM, K.P., A.B. Cua, and H.I. Maibach, Skin aging - effect on transepidermal water-loss, stratum-corneum hydration, skin surface pH and casual sebum content. *Archives of Dermatology*, 1991. **127**(12): p. 1806-1809.
39. ZHAI, H.B. and H.I. Maibach, Skin occlusion and irritant and allergic contact dermatitis: an overview. *Contact Dermatitis*, 2001. **44**(4): p. 201-206.
40. HULL, W., Heat-enhanced transdermal drug delivery: a survey paper. 2002.
41. GRUBAUER, G., et al., Lipid-content and lipid type as determinants of epidermal permeability barrier. *Journal of Lipid Research*, 1989. **30**(1): p. 89-96.
42. GOYAL, S., Novel anti-inflammatory topical gels. *International Journal of Pharmaceutical and Biological Archives*, 2011. **2**: p. 1087-1094.
43. CONVENTION, T.U.S.P., Topical and Transdermal Drug Products - Product Quality Tests. 2013.
44. HEYNEMAN, C.A., C. Lawless-Liday, and G.C. Wall, Oral versus topical NSAIDs in rheumatic diseases - A comparison. *Drugs*, 2000. **60**(3): p. 555-574.
45. KAUFMAN, D.W., et al., Recent patterns of medication use in the ambulatory adult population of the United States - The Slone survey. *Jama-Journal of the American Medical Association*, 2002. **287**(3): p. 337-344.
46. VINOD Singh and H. Sharma, Topical non steroidal anti-inflammatory drug (NSAIDs) microemulsions: Rationale, review and future prospective. 2014.
47. ChemSpider - Search and share Chemistry Ibuprofen. Available from <http://www.chemspider.com/Chemical-Structure.3544.html>. Accessed on 04/06/2016.
48. PubChem - Open Chemistry Database. Ibuprofen | C₁₃H₁₈O₂ . Available from <https://pubchem.ncbi.nlm.nih.gov/compound/ibuprofen> Accessed on 04/06/2016.
49. CAN, A.S., et al., Optimization and Characterization of Chitosan Films for Transdermal Delivery of Ondansetron. *Molecules*, 2013. **18**(5): p. 5455-5471.
50. JONES, D.S., A.D. Woolfson, and A.F. Brown, Textural analysis and flow rheometry of novel, bioadhesive antimicrobial oral gels. *Pharmaceutical Research*, 1997. **14**(4): p. 450-457.
51. VITORINO, C., et al., Design of a dual nanostructured lipid carrier formulation based on physicochemical, rheological, and mechanical properties. *Journal of Nanoparticle Research*, 2013. **15**(10).

52. GUTSCHKE, E., et al., Adhesion testing of transdermal matrix patches with a probe tack test - In vitro and in vivo evaluation. *European Journal of Pharmaceutics and Biopharmaceutics*, 2010. **75**(3): p. 399-404.
53. FOEGEDING, E.A. and M.A. Drake, Invited review: Sensory and mechanical properties of cheese texture. *Journal of Dairy Science*, 2007. **90**(4): p. 1611-1624.
54. PADULA, C., et al., Bioadhesive film for the transdermal delivery of lidocaine: in vitro and in vivo behavior. *Journal of Controlled Release*, 2003. **88**(2): p. 277-285.
55. CONVENTION, T.U.S.P. Topical and Transdermal Drug Products. 2009.
56. Vertical Glass Diffusion Cell - Franz Cells. Available from <http://www.ses-analysesysteme.de> Access on 08/06/2016.
57. SILVA, S.M.C., et al., Aggregation and gelation in hydroxypropylmethyl cellulose aqueous solutions. *Journal of Colloid and Interface Science*, 2008. **327**(2): p. 333-340.
58. HANDBOOK of Pharmaceutical Excipients. 6^a edition ed. 2009: PhP.
59. PONS, M. and S.M. Fiszman, Instrumental texture profile analysis with particular reference to gelled systems. *Journal of Texture Studies*, 1996. **27**(6): p. 597-624.
60. HURLER, J., et al., Improved texture analysis for hydrogel characterization: Gel cohesiveness, adhesiveness, and hardness. *Journal of Applied Polymer Science*, 2012. **125**(1): p. 180-188.
61. SOLTANPOUR, S. and A. Jouyban, Solubility of Acetaminophen and Ibuprofen in Binary and Ternary Mixtures of Polyethylene Glycols 200 and 400, Propylene Glycol, and Water at 25 degrees C. *Chemical Engineering Communications*, 2014. **201**(12): p. 1606-1619.
62. BOLOURCHIAN, N., M.M. Mahboobian, and S. Dadashzadeh, The effect of PEG molecular weights on dissolution behavior of simvastatin in solid dispersions. *Iranian journal of pharmaceutical research : IJPR*, 2013. **12**(Suppl): p. 11-20.
63. COSTA, P. and J.M. Sousa Lobo, Modeling and comparison of dissolution profiles *European Journal of Pharmaceutical Sciences* 2001. **13**: p. 123-133.
64. PEPPAS, N.A., I. Commentary on an exponential model for the analysis of drug delivery: Original research article: a simple equation for description of solute release: I II. Fickian and non-Fickian release from non-swellable devices in the form of slabs, spheres, cylinders or discs, 1987. *Journal of controlled release : official journal of the Controlled Release Society*, 2014. **190**: p. 31-2.
65. LIN, S.Y., C.J. Lee, and Y.Y. Lin, Drug-polymer interaction affecting the mechanical-properties, adhesion strength and release kinetics of piroxicam-loaded Eudragit-E films plasticized with different plasticizers. *Journal of Controlled Release*, 1995. **33**(3): p. 375-381.
66. WITTAYA-AREEKUL, S., C. Prahsarn, and S. Sungthongjeen, Development and in vitro evaluation of Chitosan-Eudragit RS 30D composite wound dressings. *AAPS PharmSciTech*, 2006. **7**(1): p. E30-E30.

67. KOUCHAK, M., S. Handali, and B. Naseri Boroujeni, Evaluation of the Mechanical Properties and Drug Permeability of Chitosan/Eudragit RL Composite Film. *Osong public health and research perspectives*, 2015. **6**(1): p. 14-9.
68. IRFANI, G. and R. Sunilraj, Design and Evaluation of Transdermal Drug Delivery System of Valsartan Using Glycerine as Plasticizer 2011. **3**(2): p. 185-192.
69. GUY, R. and J. Hadgraft, *Transdermal Drug Delivery*. 2 ed. 2003.
70. EMA. Guidelines on quality of transdermal patches. Available from: http://www.ema.europa.eu/docs/en_GB/document_library/Scientific_guideline/2014/12/WC500179071.pdf. Accessed on 4/07/2016.